



ECT\*



EUROPEAN CENTRE FOR THEORETICAL STUDIES  
IN NUCLEAR PHYSICS AND RELATED AREAS

TRENTO, ITALY

Institutional Member of the ESF Expert Committee NuPECC

# *Total Inelastic Cross Section at LHC*

Sara Valentineti, INFN and Univ. of Bologna (Italy)

On behalf of ATLAS and CMS

*LC13 Workshop, ECT\*, Villa Tambosi, Villazzano (TN), 16-20 Sep 2013*

# Outline

- Introduction on Inelastic and Diffractive Physics;
- Measurements in **CMS**, **total inelastic cross section**:
  - ➔ single side counting: CMS PAS QCD-11-002;
  - ➔ pile up counting: CMS PAS FWD-11-001;  
*Measurement of the Inelastic Proton-Proton Cross Section at  $\sqrt{s} = 7$  TeV (Phys. Lett. B 722 (2013) 5-27)*
- Measurements in **ATLAS**:
  - total inelastic cross section** ➔ single side counting;  
*Measurement of the Inelastic pp Cross Section at  $\sqrt{s} = 7$  TeV with the ATLAS Detector (Nature Comm. 2 (2011) 463);*
  - differential inelastic cross section** ➔ rapidity gap counting;  
*Rapidity Gap Cross Sections measured with the ATLAS Detector in pp Collisions at  $\sqrt{s} = 7$  TeV (Eur. Phys. J.C72 (2012) 1926);*
- Discussion of results and comparison with theory.

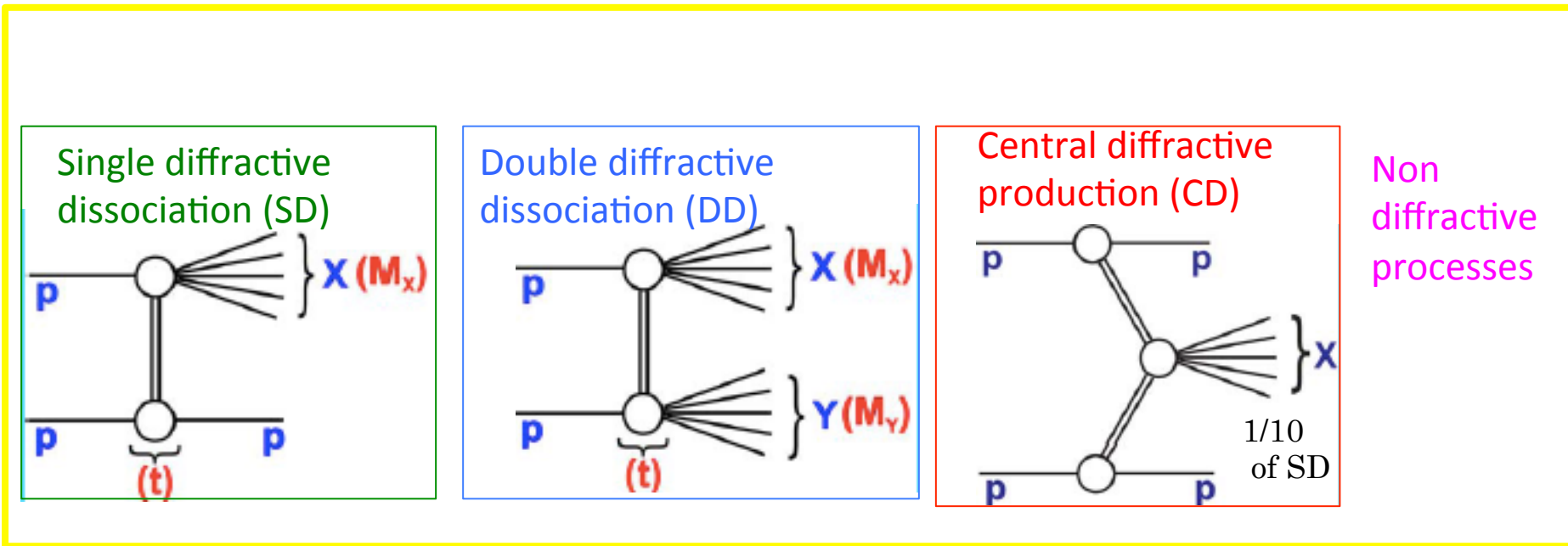
# The Total pp Cross Section

Total pp cross section composed by different contributions:

$$\sigma_{\text{tot}} = \sigma_{\text{EL}} + \underbrace{\sigma_{\text{SD}} + \sigma_{\text{DD}} + \sigma_{\text{CD}} + \sigma_{\text{ND}}}_{\text{INELASTIC}}$$

Elastic scattering

*INELASTIC*

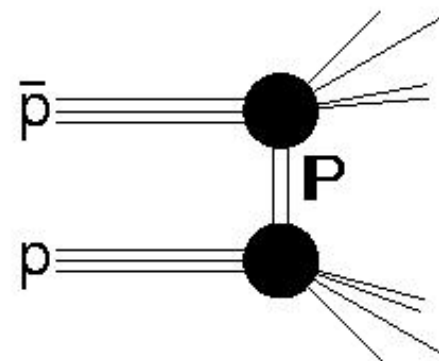


At LHC energy: - 20% elastic, 80% inelastic;  
 - diffractive contribution  $\sigma_{\text{D}}/\sigma_{\text{inel}} \approx 0.2 - 0.3$ .

# Theoretical Definition of Diffractive Physics

## No unique definition of diffraction processes

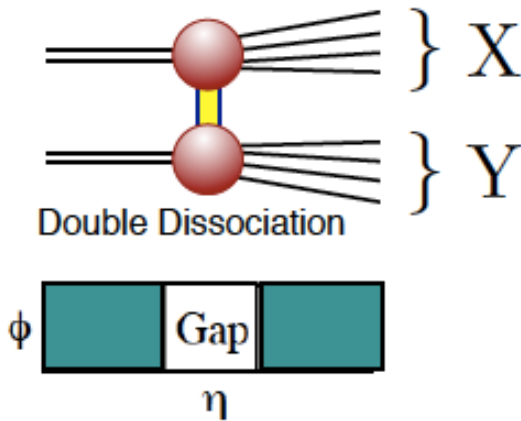
1. Interactions mediated by t-channel exchange of object (ladder of gluons) with the quantum numbers of the vacuum, i.e. color singlet exchange called “Pomeron”.
2. Interactions where the beam particles emerge intact or dissociated into low mass states.



Diffractive physics not completely described by QCD.

Phenomenological approaches based on QCD + different models implemented in MC simulations → importance to compare models to data.

# Diffractive Dissociation



Experimentally:

Kinematic variables:

- $t$ , the 4-momentum exchanged at the proton vertex;
- the mass of diffractive system,  $M_X > M_Y$  or  $\xi_{X(Y)} \equiv M_{X(Y)}^2/s$  (fractional squared momentum loss)

Total cross section not directly measured by ATLAS and CMS yet.

- Direct measurements of  $M_{X(Y)}$  difficult: produced particles escape along the beam-pipe.
- ATLAS/CMS central detectors sensitive to high mass diffraction  
 → low mass diffractive states not directly observable.

Diffractive processes lead to final state particles separated by large rapidity gaps: region of no activity (particle production suppressed).

Link between  $M_X$  and rapidity gap  $\Delta \eta$  (for SD):  $\Delta \eta \approx \ln s/M_X^2 = -\ln \xi_X$ .

# Analysis Strategy

Limits due to detector acceptance  $\rightarrow \xi = M_X^2/s > 5 \times 10^{-6}$  ( $M_X > 15.7$  GeV)

Inelastic cross section measured in limited kinematic range then extrapolated at full range using MC.

## Measurements:

CMS: total inelastic cross section

ATLAS: total and differential  
inelastic cross section

## Methods:

CMS: 1) hit counting in  
calorimeters,  
2) vertex counting in  
tracker;

ATLAS: hit counting in scintillator  
counters;

## Statistics:

CMS: 7 runs in 2010

$\mu \in [0.007; 0.1]$

High statistics, systematic  
effect due to pile up.

ATLAS: single fill in 2010

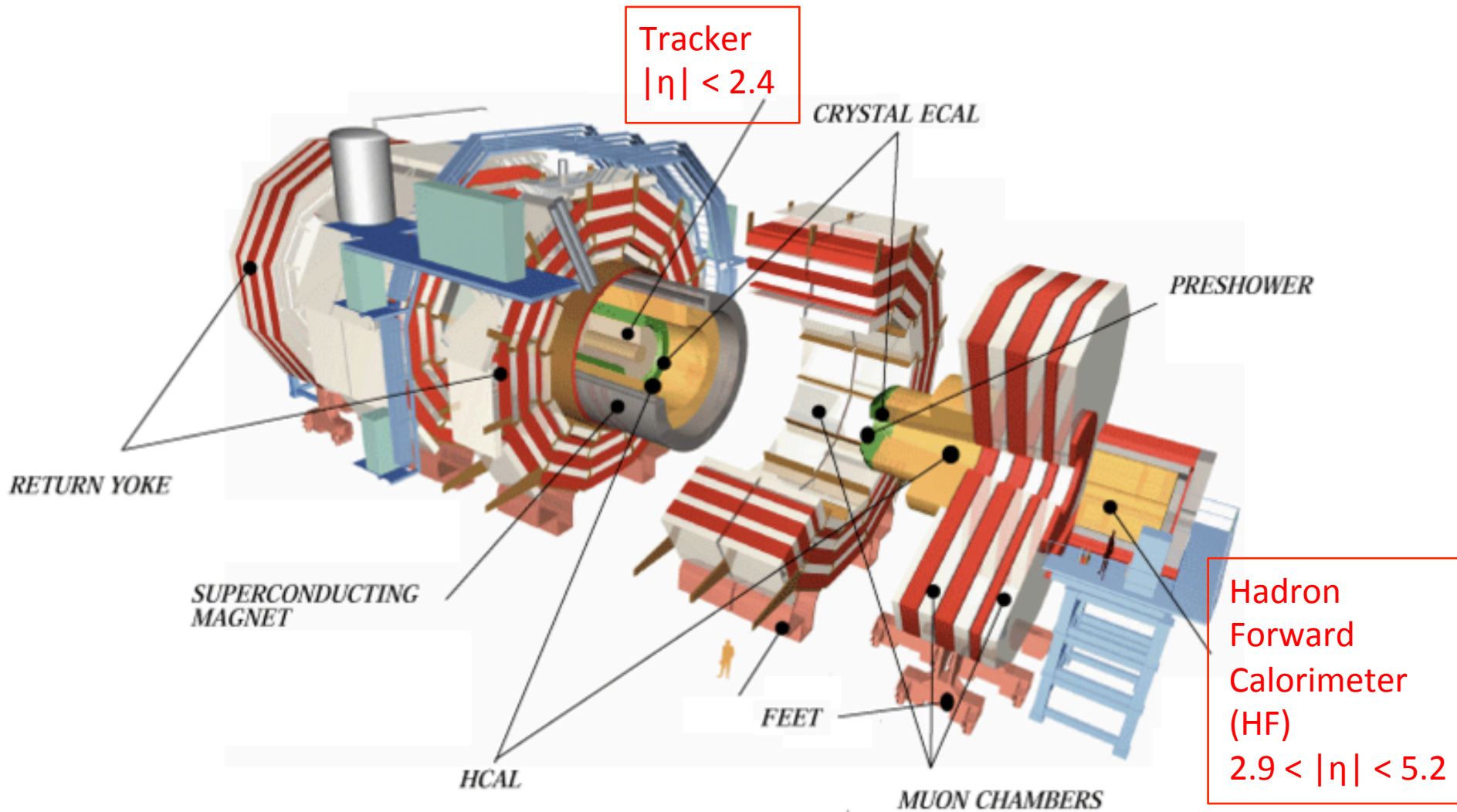
$\mu = 0.01$

Low statistics,  
pile up removal.

Measurement of the Inelastic Proton-  
Proton Cross Section at  $\sqrt{s} = 7\text{TeV}$   
with CMS

*(Phys. Lett. B 722 (2013) 5-27)*

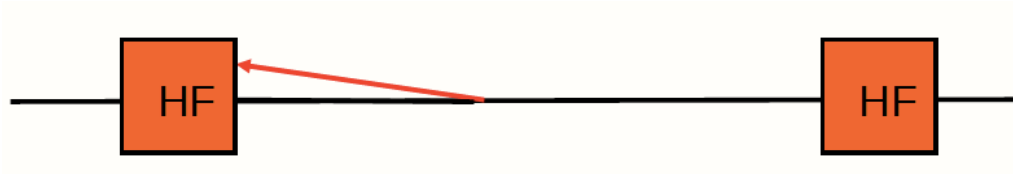
# CMS Detector





## Single Side Counting (CMS PAS QCD-11-002)

Number of events with at least 5 GeV of energy in either of the two hadron forward calorimeters (HF) counted.

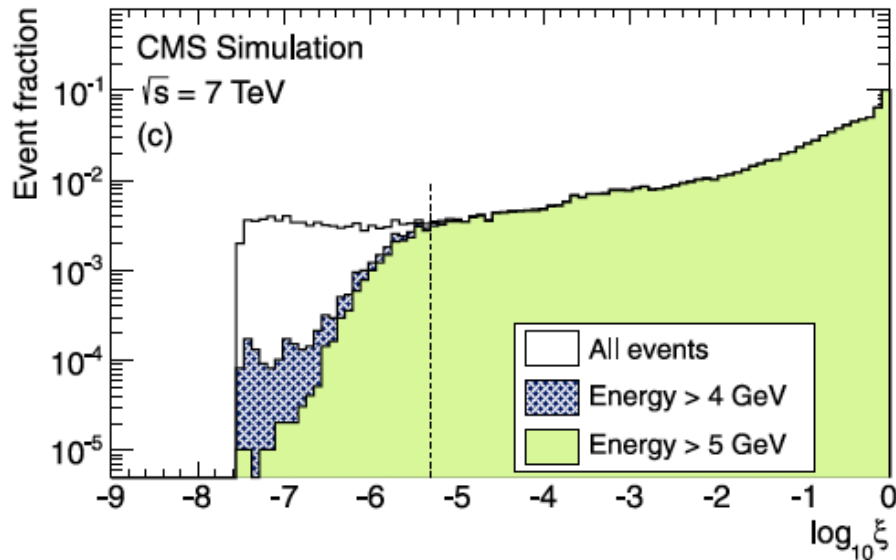


Three triggers: 1) coincidence trigger (for pp events);  
2) single bunch trigger (for unpaired bunches);  
3) random empty trigger (for detector noise).

HF acceptance outside tracker acceptance → impossible to separate multiple inelastic events in the same bunch crossing → pile up correction needed.

# Event Selection Efficiency

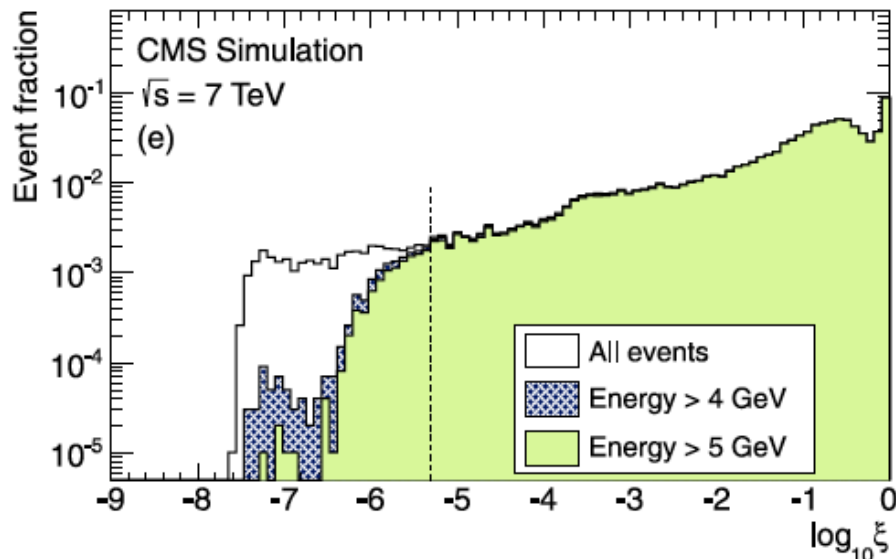
PYTHIA 8



Events with small  $\xi$  can escape detection due to detector acceptance

→ event selection efficiency studied as function of  $\xi$  for different MC generators: PYTHIA6, PYTHIA8, PHOJET.

PHOJET



For  $\xi > 5 \times 10^{-6}$  CMS has more than 98% efficiency of detection.

ATLAS results are also available for  $\xi > 5 \times 10^{-6}$  → direct comparison

# Cross Section Measurement

$$\sigma_{inel}(\xi > 5 * 10^{-6}) = \frac{N_{inel} (1 - f_{\xi})(1 + f_{pu})}{\epsilon_{\xi} L_{int}}$$

$N_{pp} - N_{bkg}$  (points to  $N_{inel}$ )  
 Detector and event selection efficiency ( $\approx 98\%$  at 5 GeV for PYTHIA/PHOJET) (points to  $\epsilon_{\xi}$ )  
 Integrated lumi  $2.78 \mu\text{b}^{-1}$  (points to  $L_{int}$ )  
 Contamination: fraction of events passing the selection but produced at  $\xi < 5 * 10^{-6}$  ( $\approx 0.02/0.01$  for PYTHIA/PHOJET at 5 GeV) (points to  $f_{\xi}$ )  
 Pile up correction (more than one collisions counted as one) (points to  $f_{pu}$ )

The number of collisions per trigger follows a Poisson statistics:

$$P(n, \lambda) = \frac{\lambda^n e^{-\lambda}}{n!}$$

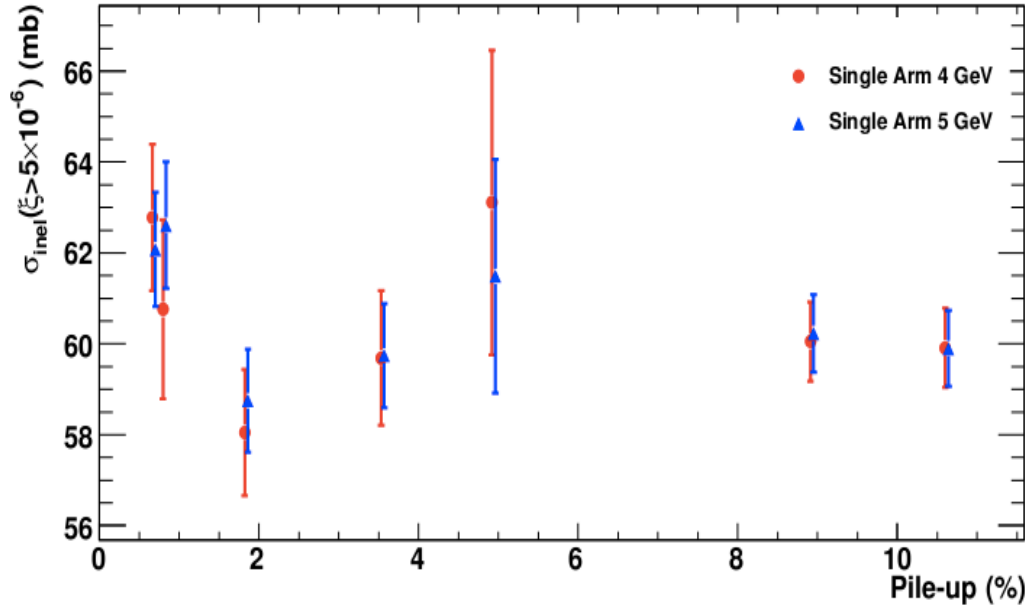
$\lambda$  = mean number of interactions with  $E_{HF} > 5\text{GeV}$ .

The fraction of overlapping events is evaluated from data for 7 different luminosity conditions:

$$f_{pu} = \frac{\sum_{n=2}^{\infty} P(n, \lambda)}{\sum_{n=1}^{\infty} P(n, \lambda)} = \frac{1 - (1 + \lambda)e^{-\lambda}}{1 - e^{-\lambda}} \sim \frac{\lambda}{2} - \frac{\lambda^2}{12} + \mathcal{O}(\lambda^3).$$

For each  $f_{pu}$ , a value of  $\sigma_{inel}(\xi > 5 * 10^{-6})$  is provided.

# Inelastic pp Cross Section @ 7 TeV



Averaging  $\sigma$  values obtained under 7 (low) pile-up conditions:

$$\sigma_{inel}^{pp}(\xi > 5 * 10^{-6}) = 60.2 \pm 0.2(stat.) \pm 1.1(syst.) \pm 2.4(lumi)mb$$

Total inelastic cross section extrapolated to the full kinematic range using six additional MC models.

Extrapolation factor (only MC dependent) averaged over models:  $1.071 \pm 0.025$

$$\sigma_{inel}^{pp}(7TeV) = 64.5 \pm 0.2(stat.) \pm 1.1(syst.) \pm 2.6(lumi) \pm 1.5(extr.)mb$$

Systematic source	Uncertainty on $\sigma_{inel}$	Change in $\sigma_{inel}$
Run-to-run variation	$\pm 0.8$ mb	$\pm 1.3\%$
Selection efficiency	$\pm 0.6$ mb	$\pm 1.0\%$
Contamination from $\xi < 5 \times 10^{-6}$	$\pm 0.3$ mb	$\pm 0.5\%$
HF tower exclusion	$\pm 0.3$ mb	$\pm 0.4\%$
HF energy threshold	$\pm 0.1$ mb	$\pm 0.2\%$
Total (in quadrature)	$\pm 1.1$ mb	$\pm 1.8\%$

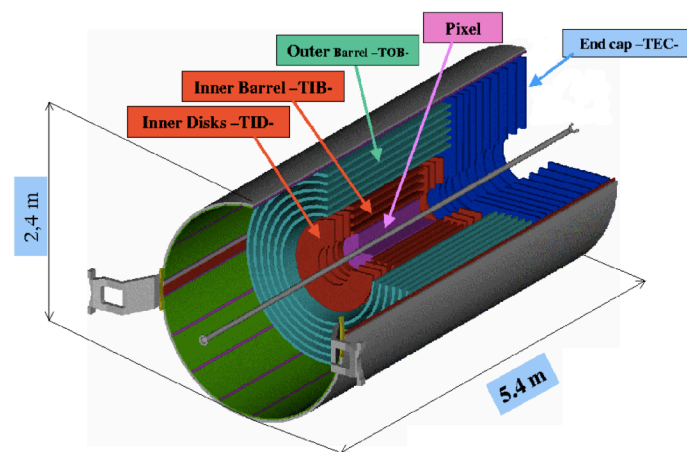
# Vertex Counting Method (CMS PAS FWD-11-001)

Estimation of the inelastic cross section by counting event vertices.

It relies on accuracy of tracking system not on MC simulations.

Two samples triggered by tracking system:

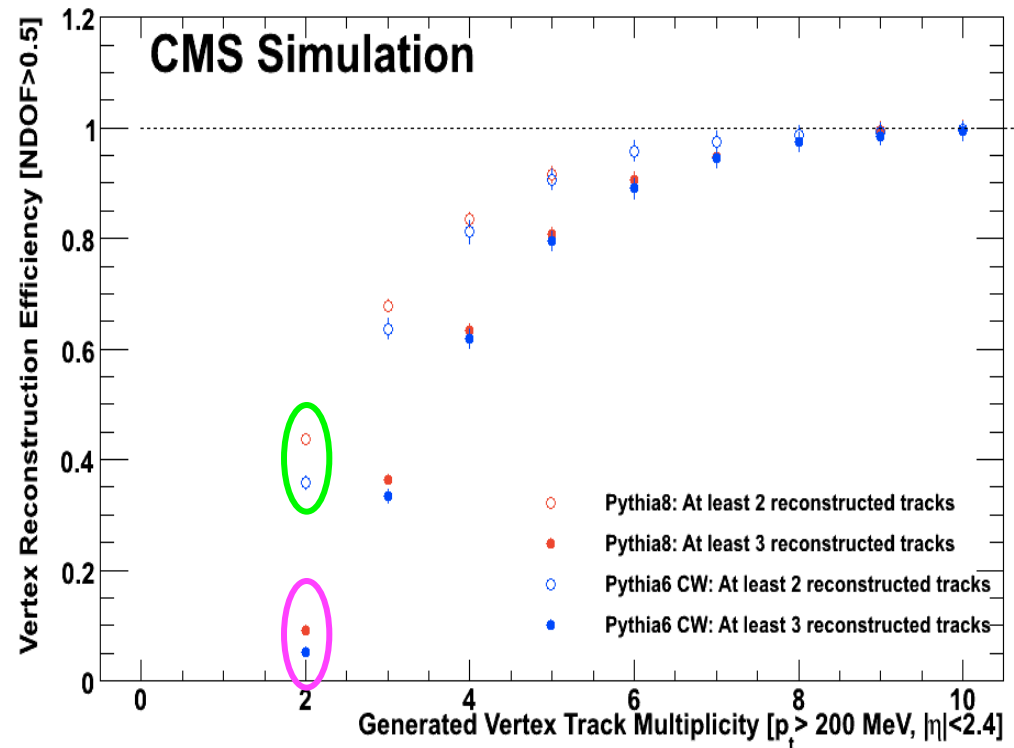
- 1) single-muon candidate events (for analysis);
- 2) inclusive sample of two-electron candidate events (for systematic check on the trigger choice).



Specific trigger requirements not important because their efficiencies do not depend on number of pile up.

# Vertex Definition

- Quality cuts on vertex:
  - **>1, >2 or >3 tracks** with  $p_T > 200$  MeV in  $|\eta| < 2.4 \rightarrow$  **3 set of events**;
  - each track should have at least 2 pixel hits and 5 strip hits in the tracker;
  - the vertex should pass an overall quality cut on track fit:
- Vertex efficiency derived from PYTHIA simulation ( $\sim 40\%$  for a 2 tracks vertex (green) and  $\sim 20\%$  for a 3 tracks vertex (pink))
- Inefficiencies due to:
  - fake vertices (real secondary vertices and fake secondary vertices);
  - reconstruction inefficiencies.



# Analysis Strategy

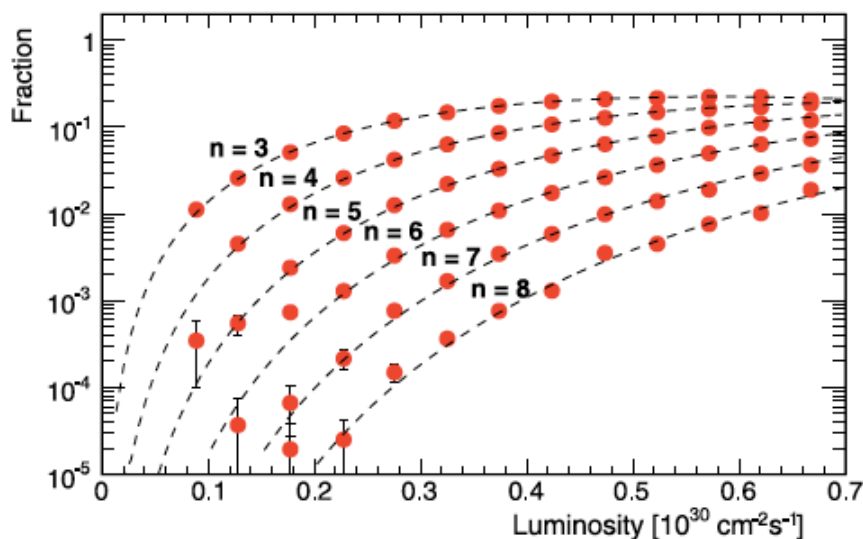
$$P(n_{pileup}) = \frac{(L_{inst} * \sigma)^{n_{pileup}}}{n_{pileup}!} e^{-(L_{inst} * \sigma)}$$

Idea: use the measured probability of having  $n$  (0 to 8) inelastic pp interactions each producing a vertex for different luminosities to evaluate  $\sigma_{inel}$  from fit.

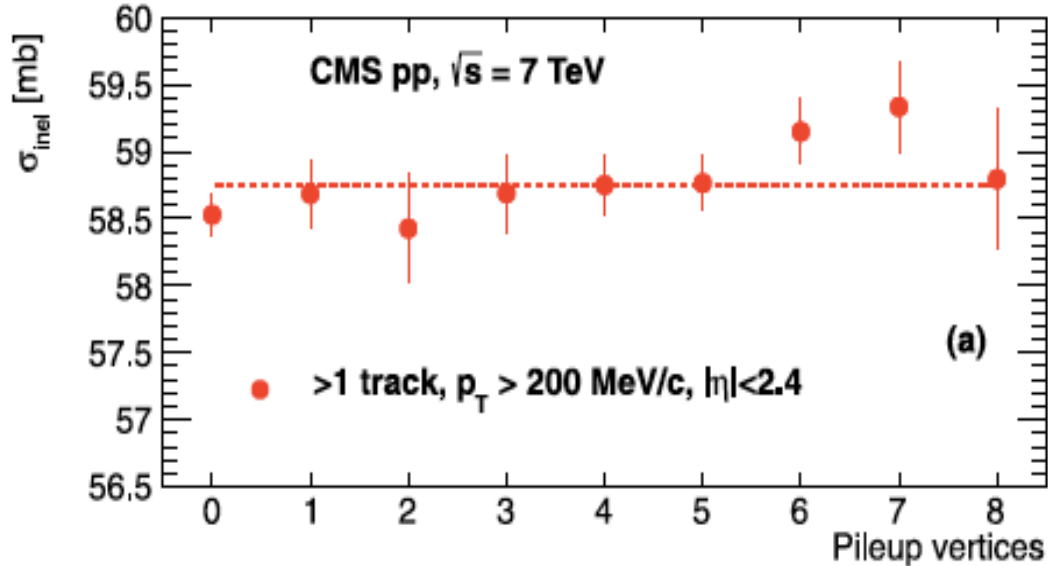
For each sample:

- 1) Count the number of pile-up events for a luminosity value:
  - number of vertices in the event counted for any given bunch crossing;
- 2) Bin-by-bin MC corrections of the distribution of number of visible vertices for various effects;
- 4) Fit the probability of having 0 to 8 pile-up events as a function of luminosity with a Poisson curve → 9 values of  $\sigma_{visible}$  obtained.

Fraction of pp events with  $n$  pile up vertices



# Total Visible Inelastic pp Cross Section @ 7 TeV



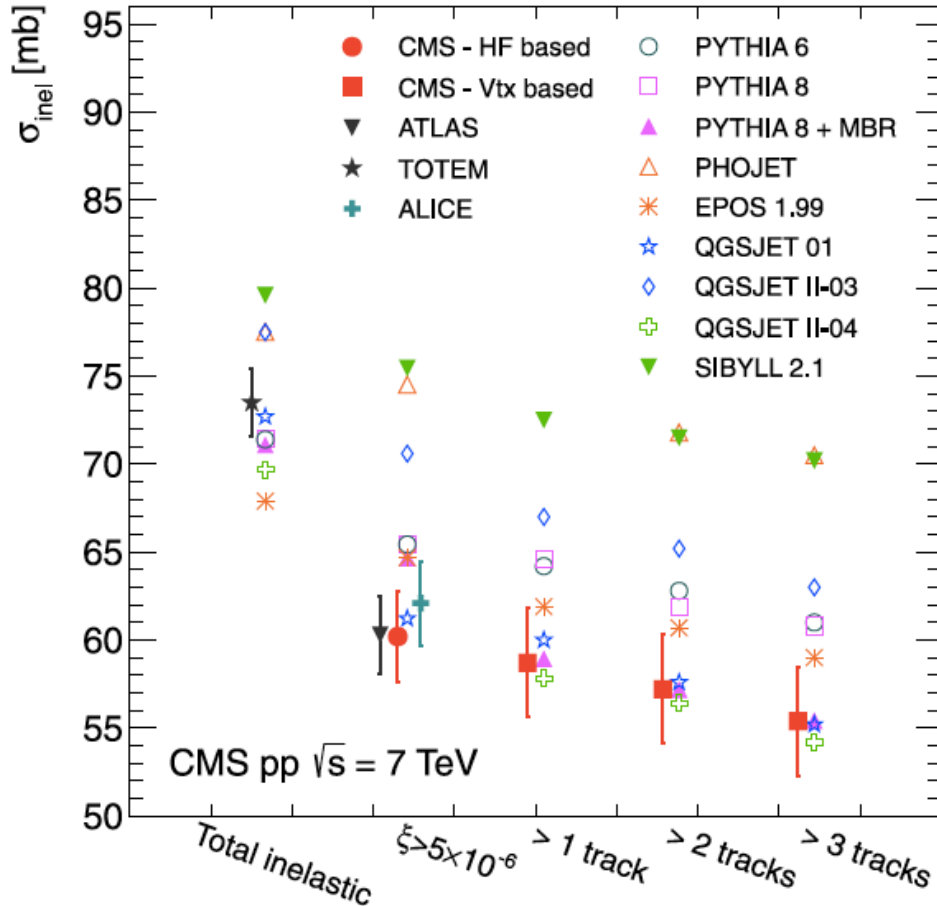
Total visible inelastic cross section obtained averaging the 9 values of visible cross section, each obtained fitting the pile up distribution.

Analysis repeated for the three sets of events:

Measurement	Result
$\sigma_{\text{inel}}(>1 \text{ track})$	$[58.7 \pm 2.0(\text{syst.}) \pm 2.4(\text{lum.})]$ mb
$\sigma_{\text{inel}}(>2 \text{ tracks})$	$[57.2 \pm 2.0(\text{syst.}) \pm 2.4(\text{lum.})]$ mb
$\sigma_{\text{inel}}(>3 \text{ tracks})$	$[55.4 \pm 2.0(\text{syst.}) \pm 2.4(\text{lum.})]$ mb



# Total Inelastic pp Cross Section @ 7 TeV



Additional MC models used:  
PYTHIA6, PYTHIA8,  
PHOJET, SIBYLL, EPOS and  
QGSJET-II.

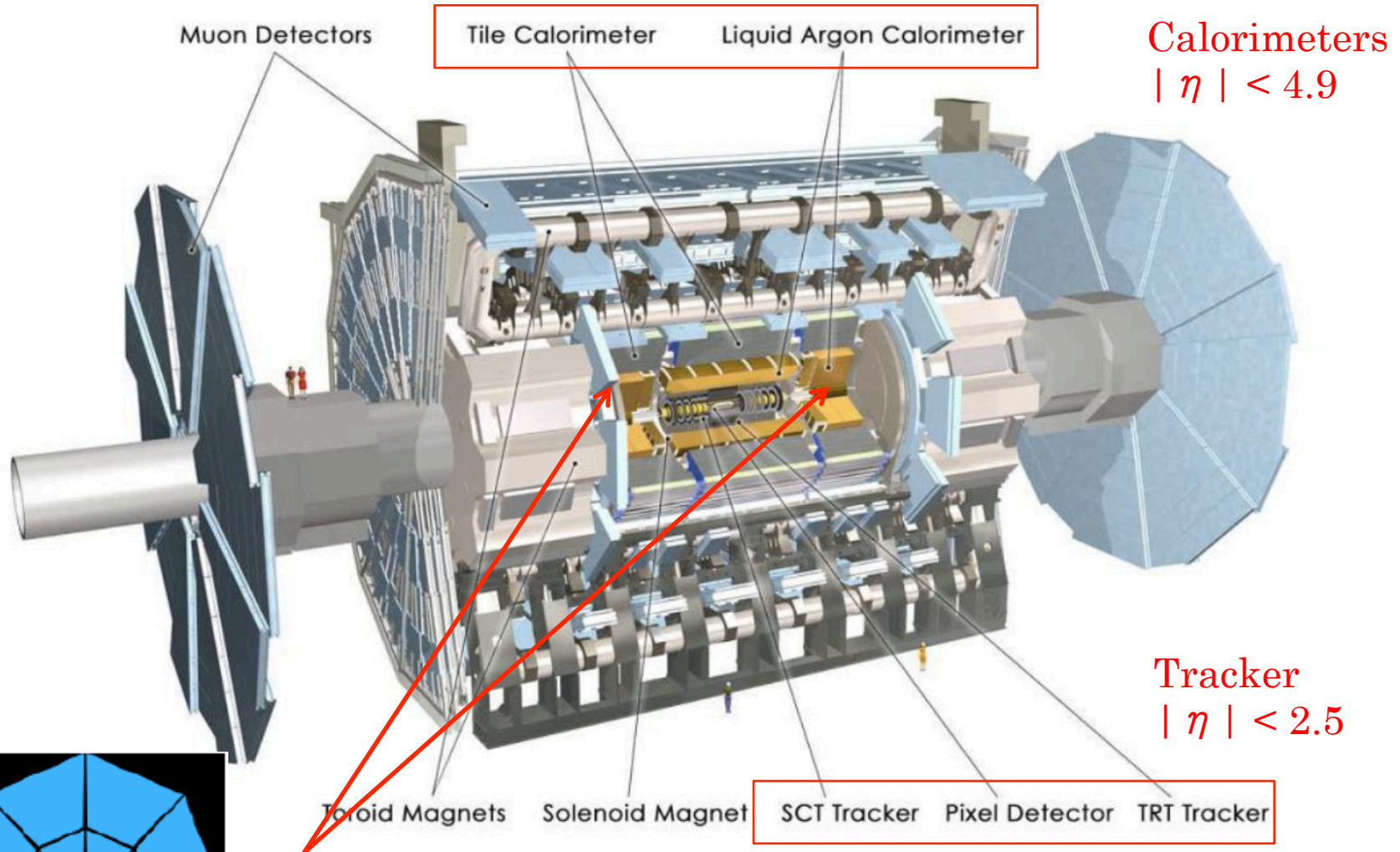
Similar trend for the measured  
cross sections but substantial  
differences in the expectation of  
the total inelastic pp cross  
section.

$$\sigma_{inel}^{pp}(7\text{TeV}) = 68.0 \pm 2.0(\text{syst.}) \pm 2.4(\text{lumi})$$

$$\pm 4.0(\text{extr.})\text{mb}$$

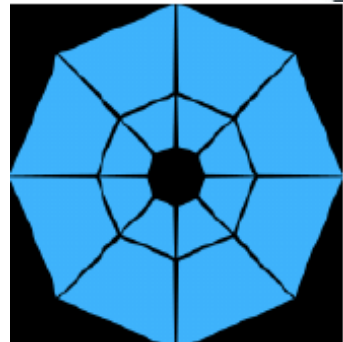
Systematic source	Uncertainty on $\sigma_{inel}$
Vertex reconstruction efficiency	$\pm 1.4$ mb
Longitudinal position of vertex	$\pm 0.1$ mb
Vertex quality	$\pm 0.7$ mb
Minimum distance between vertices	$\pm 0.1$ mb
Transverse position of vertex	$\pm 0.3$ mb
Different sets of data	$\pm 0.9$ mb
Range of luminosity used in fit	$\pm 0.2$ mb
Reweighting MC track distribution	$\pm 0.2$ mb
<b>Total (in quadrature)</b>	<b><math>\pm 2.0</math> mb</b>

# ATLAS Detector



## Minimum Bias Trigger Scintillator (MBTS) $2.1 < |\eta| < 3.8$

16 plastic scintillators on each side read out by fibers+PMTs.



# Measurement of the inelastic pp cross section at $\sqrt{s}=7$ TeV with ATLAS

(Nature Comm. 2 (2011), April 2011)

Minimum Bias Trigger Scintillator (MBTS) counting.

Two data sample:

- 1) **inclusive** events: at least two MBTS counters above threshold on at least one side of ATLAS.
- 2) **single-sided** events: at least two MBTS hits on one side and no hits on opposite side.

# Cross Section Measurement

MBTS triggered events -  
Background (unpair bunches)

Contamination: fraction of events passing the selection but produced at  $\xi < 5 \cdot 10^{-6}$

Limit due to detector acceptance

$$\sigma_{inel}(\xi > 5 \cdot 10^{-6}) = \frac{(N - N_{bkg})}{\epsilon_{trigg} * L_{int}} \times \frac{1 - f_{\xi < 5 \cdot 10^{-6}}}{\epsilon_{sel}}$$

Trigger efficiency  $\approx 99.98\%$

Integrated lumi =  $20 \mu b^{-1}$   
(calibrating with vdM scans)

Offline event selection efficiency  
(50% for  $\xi = 5 \cdot 10^{-6}$ ,  
 $\approx 100\%$  for  $\xi > 10^{-5}$ )

$N$ ,  $N_{bkg}$ ,  $\epsilon_{trigg}$ ,  $L_{int}$  obtained from data.

$\epsilon_{sel}$ ,  $f_{\xi < 5 \cdot 10^{-6}}$  obtained from tuned MC simulation: variety of models

→ large uncertainty due to model dependence.

To reduce MC uncertainty, the ratio of single sided to inclusive events

$R_{ss} = N_{SS} / N_{incl}$  is measured to constrain the  $f_D$  value (relative diffraction dissociation cross section):

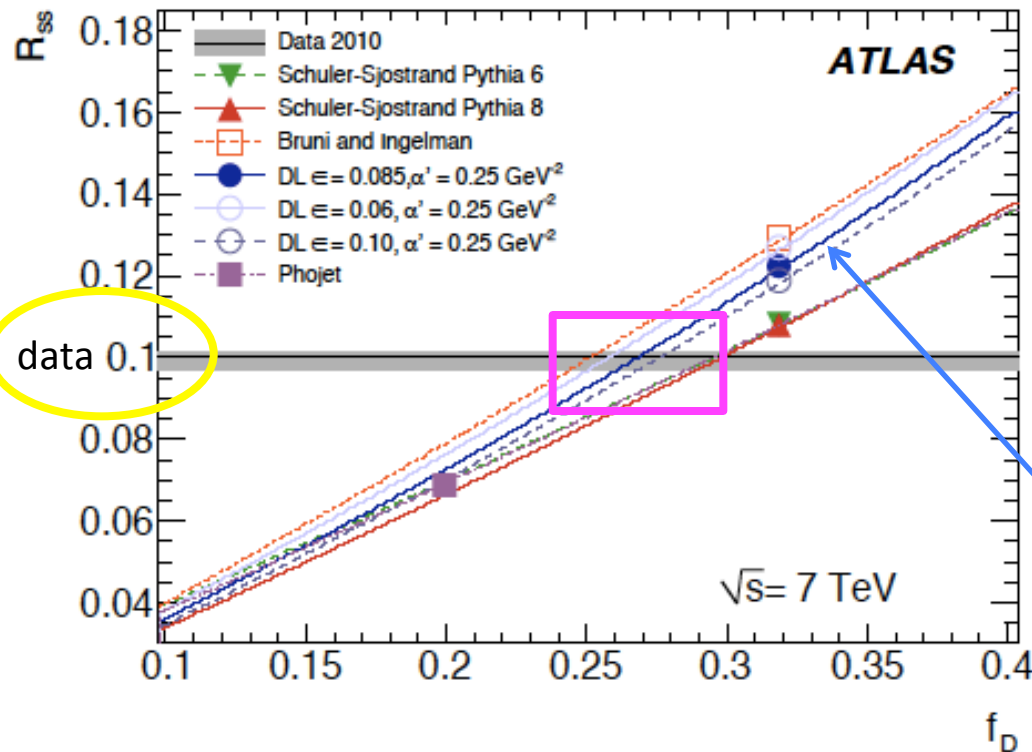
$$f_D = \frac{(\sigma_{SD} + \sigma_{DD} + \sigma_{CD})}{\sigma_{inel}}$$

# Constraining $f_D$

- Measure the ratio of single sided to inclusive events  $R_{SS}=N_{SS}/N_{incl}$

$$R_{SS} = [10.02 \pm 0.03(stat.)_{-0.4}^{+0.1}(syst.)]\%$$

- Comparison of data to different MC.
- Constrain  $f_D$  for each model by finding value that match  $R_{SS}$ .
- Different models studied for the systematics.



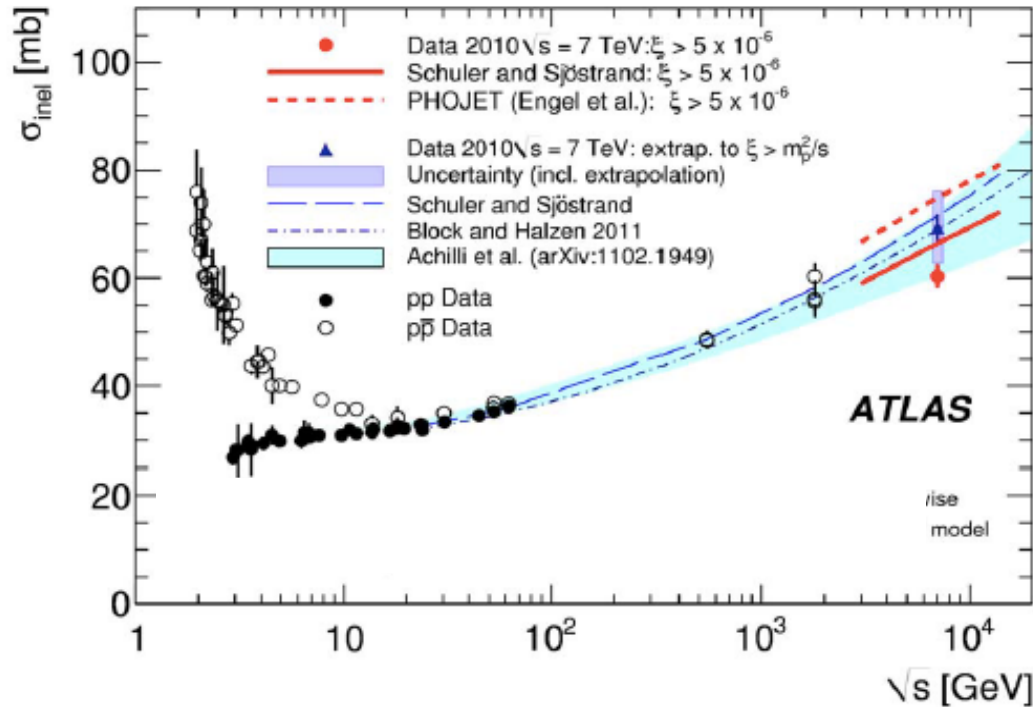
Constrain on  $f_D$ :

$$f_D = 26.9_{-1.0}^{+2.5}\%$$

Default model: PYTHIA8 with Donnachie-Landshoff  $\xi$  - dependence parametrization.

Other models give  $f_D \in [25-30]\%$

# Total Inelastic pp Cross Section @ 7TeV



Source	Uncertainty (%)
Trigger Efficiency	0.1
MBTS Response	0.1
Material	0.2
$f_D$	0.3
Beam Background	0.4
MC Multiplicity	0.4
$\xi$ distribution	0.4
Luminosity	3.4
Total	3.5

$$\sigma_{inel}^{pp}(\xi > 5 * 10^{-6}) = 60.3 \pm 0.05(stat.) \pm 0.5(syst.) \pm 2.1(lumi)mb$$

Measured  $\sigma(\xi > 5 * 10^{-6})$  lower than PYTHIA/PHOJET predictions.  
Total inelastic pp cross section extrapolated to full  $\xi$  using PYTHIA implementation of Donnachie-Landshoff model:

$$\sigma_{inel}^{pp}(7TeV) = 69.1 \pm 2.4(exp.) \pm 6.9(extr.)mb$$

Large extrapolation errors  $\rightarrow$  Important to measure it directly.

# Rapidity Gap Cross Section Measured with the ATLAS Detector in pp Collisions at $\sqrt{s}=7$ TeV

Eur. Phys. J.C72 (2012) 1926

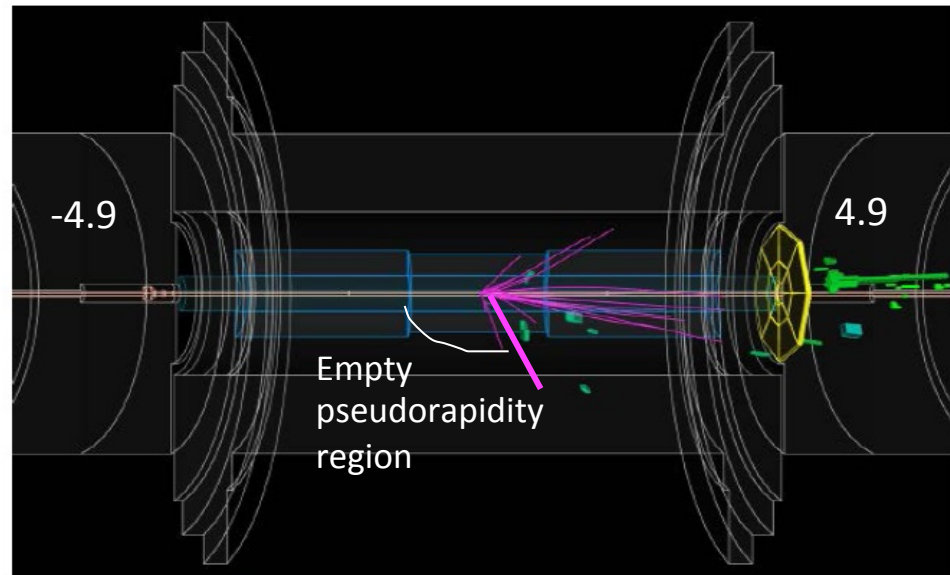
Inclusive events: at least two counters of Minimum Bias Trigger Scintillator detector (MBTS) above threshold on at least one side of ATLAS.

Select diffractive sample with large rapidity gap.

Compare  $d\sigma/d\eta$  ( $d\sigma/d\xi$ ) with various MC generators allowing to **tune MC**.

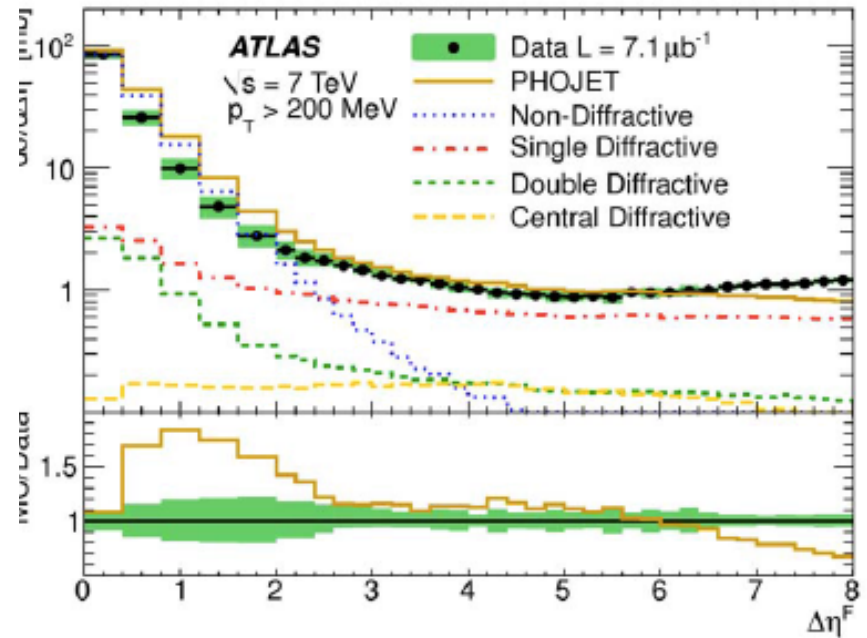
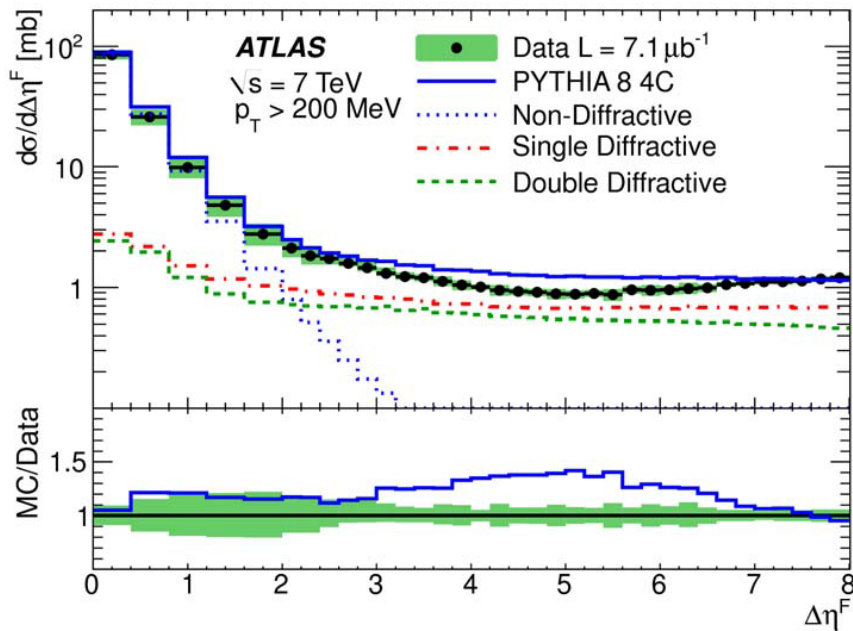
# Rapidity Gap Definition

- Pseudorapidity acceptance defined by tracker and calorimeters:  
 $-4.9 < \eta < 4.9$
- Acceptance divided in rings of unit- $\Delta\eta$  starting from  $\pm 4.9$ ;
- Activity in a  $\Delta\eta$  ring defined as either:
  - $\geq 1$  track with  $p_T > 200$  MeV  
(ID:  $|\eta| < 2.5$ )
  - $\geq 1$  calorimeter cell above noise threshold ( $2.5 < |\eta| < 4.9$ )
- Specific observable studied  
 $\Delta\eta^F =$  the larger of the two forward pseudorapidity region from  $\eta = \pm 4.9$  to the nearest track or calorimeter cluster with no ring activity.
- Data cover the range  $0 < \Delta\eta^F < 8$  (detector acceptance).  
Diffractive events : large  $\Delta\eta^F$  ( $\Delta\eta^F = \Delta\eta - 4$ )  
MC prediction:  $d\sigma/d\Delta\eta^F \sim \text{const}$



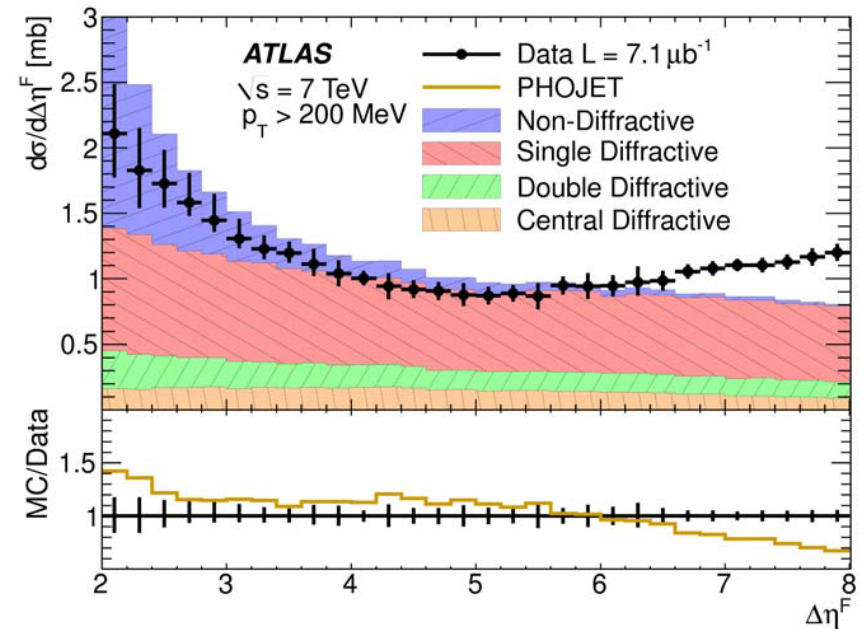
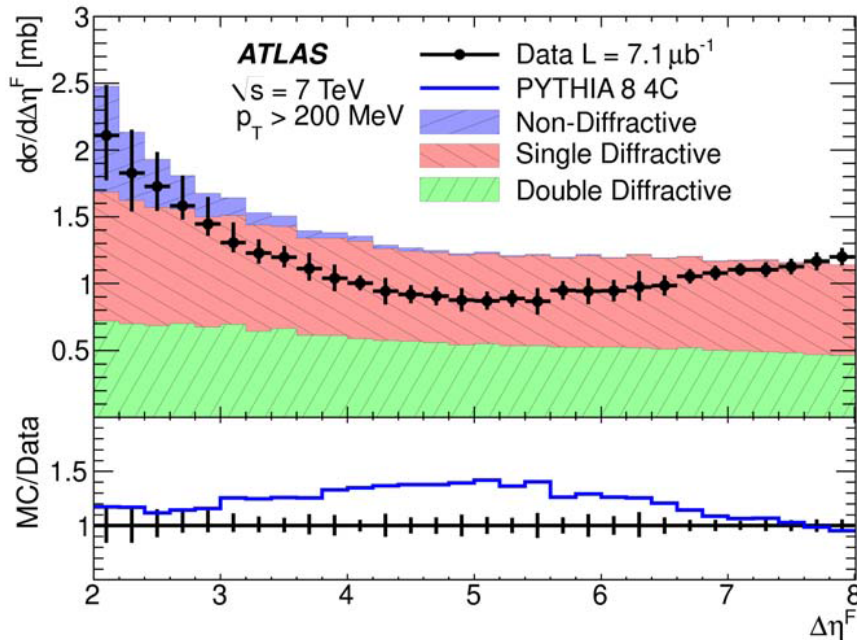


# Differential Inelastic pp Cross Section



- low  $\Delta\eta^F$  ( $<2$ ): exponential decrease due to ND contribution;
- intermediate  $\Delta\eta^F$  ( $2 < \Delta\eta^F < 5$ ) plateau due to diffractive component, ND component suppressed;
- high  $\Delta\eta^F$  ( $>5$ ): rise due to diffractive component only.

# $d\sigma_{\text{inel}}/d\Delta\eta^F$ vs Gaps for $\Delta\eta^F > 2$



No MC describes all data in all  $\Delta\eta^F$  range.

PYTHIA reproduces data better at low  $\Delta\eta^F$ , PHOJET reproduced data better at intermediate  $\Delta\eta^F$ . No MC reproduces the rise of cross section at large  $\Delta\eta^F$ .

PYTHIA:

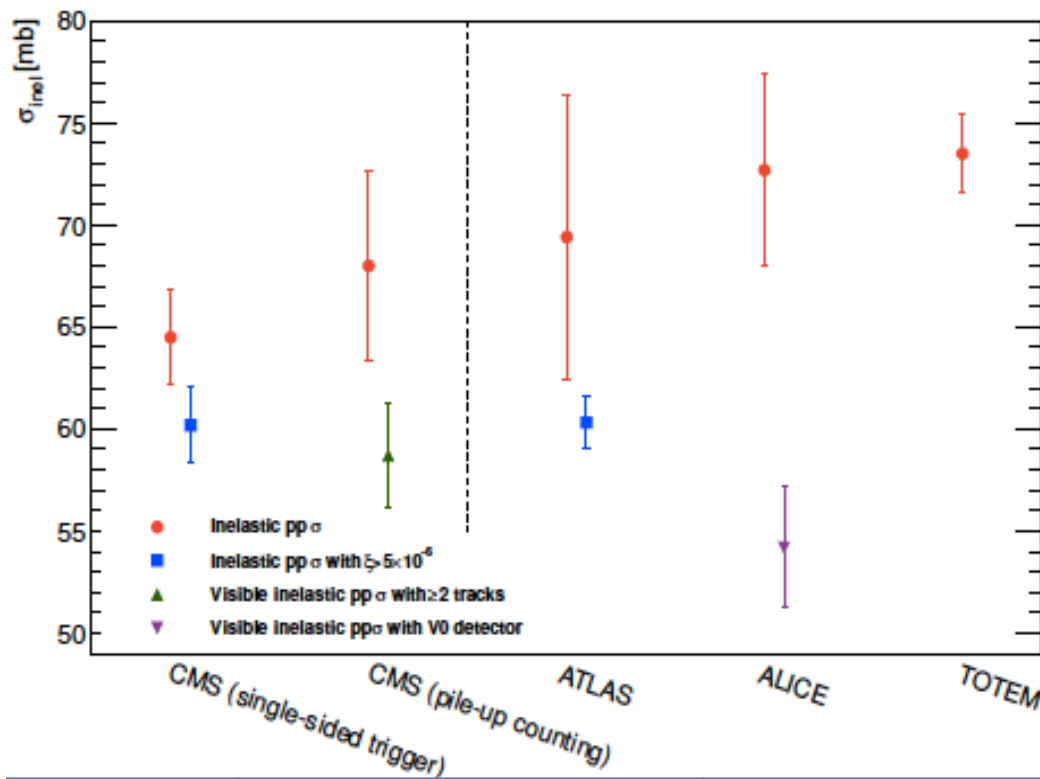
overshoot of data due to DD overestimation and missing CD components;

PHOJET:

CD contribution modeled but smaller DD contribution. Total inelastic cross section overestimated.

# Discussion of results and comparison with theory

# Comparison of $\sigma_{\text{inel}}(\text{pp})$ at $\sqrt{s} = 7\text{TeV}$



TOTEM Total inelastic pp cross section

$$\sigma_{\text{inel}} = 73.5^{+2.4}_{-1.9} \text{ mb}$$

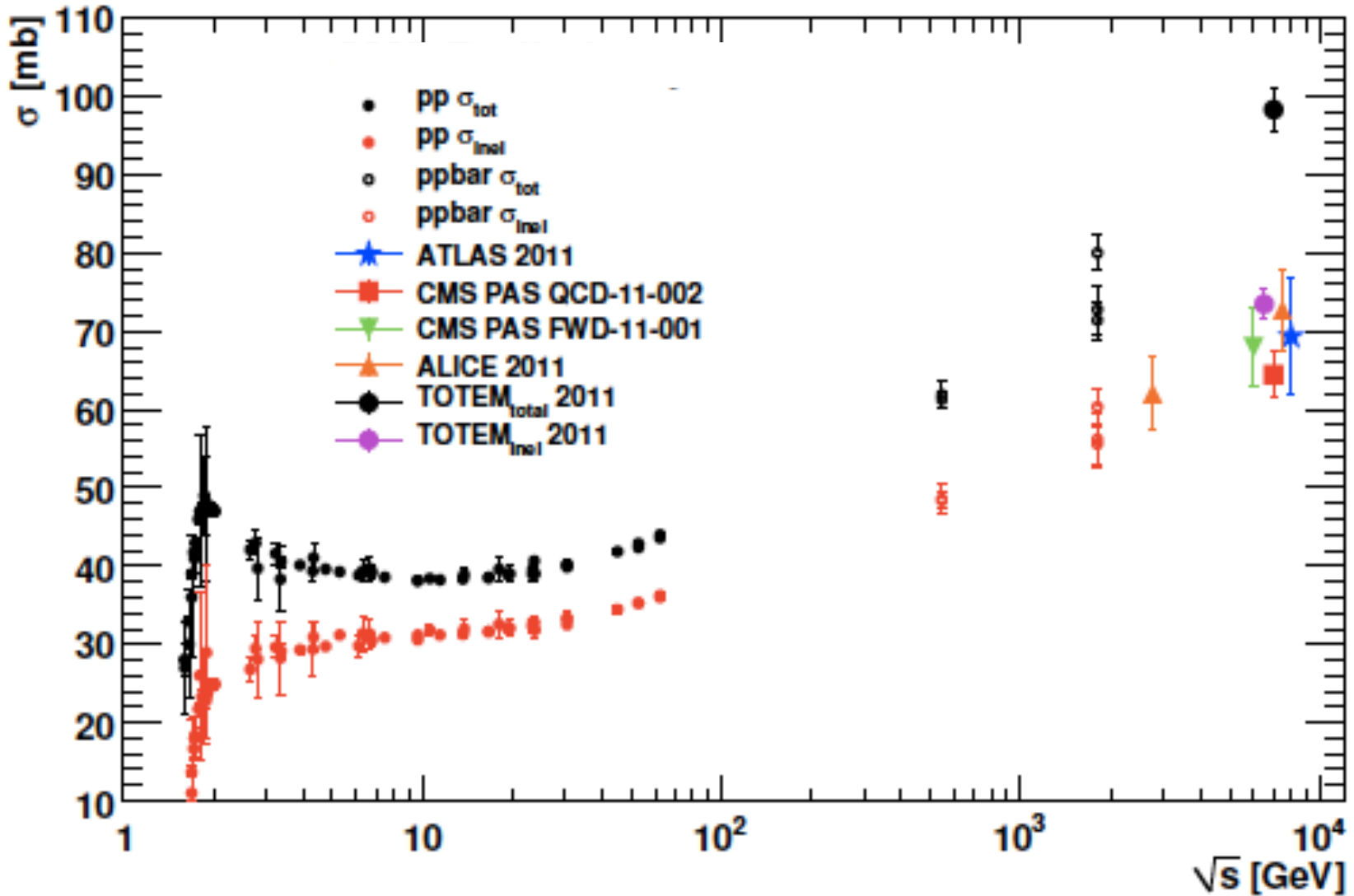
ALICE Visible pp cross section  
( $2.8 < \eta < 5.1$  &  $-3.7 < \eta < -1.7$ )

$$\sigma_{\text{inel}} = 72.7 \pm 5.2 \text{ mb}$$

ATLAS and CMS in agreement for  $\sigma_{\text{inel}}(\xi > 5 \cdot 10^{-6})$ . High uncertainties on extrapolations of total inelastic cross section due to different theoretical models.

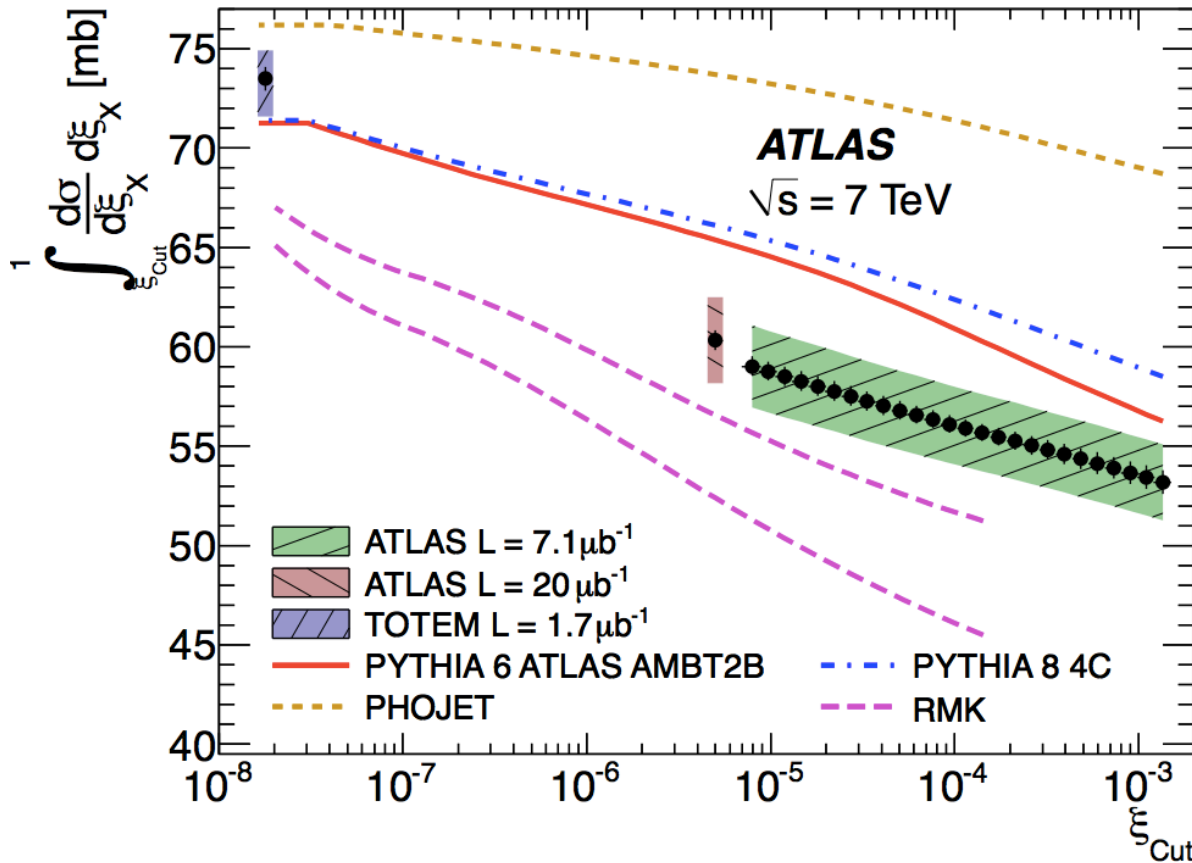
$\sigma_{\text{inel}}$ (mb)	CMS HF calorimeter	CMS Pile up	ATLAS MBTS counting
$\xi > 5 \cdot 10^{-6}$	$60.2 \pm 0.2(\text{stat}) \pm 1.1(\text{sys}) \pm 2.2(\text{lumi})$	1 track 58.7 2 track 57.2 $\pm 2.0(\text{sys}) \pm 2.4(\text{lumi})$ 3 track 55.4	$60.30 \pm 0.05(\text{stat}) \pm 0.50(\text{sys}) \pm 2.10(\text{lumi})$
Full range	$64.5 \pm 0.2(\text{stat}) \pm 1.1(\text{sys}) \pm 2.6(\text{lumi}) \pm 1.5(\text{extr})$	$68.0 \pm 2.0(\text{exp}) \pm 2.4(\text{lumi}) \pm 4.0(\text{extr})$	$69.1 \pm 2.4(\text{exp}) \pm 6.9(\text{extr})$

# Comparison of Inelastic pp Cross Section Measurements



# ATLAS vs Theory

## Differential Inelastic Cross Section Integrated for $\xi > \xi_{\text{cut}}$ vs $\xi_{\text{cut}}$



Total inelastic cross section for  $\Delta\eta^F < \Delta\eta_{\text{cut}}^F$  ( $\xi > \xi_{\text{cut}}$ ) as function of  $\xi_{\text{cut}}$

$$\log \xi_{\text{cut}} = -0.45 \Delta\eta_{F,\text{cut}} - 1.52$$

ATLAS measurements compared with different theoretical models.

Similar trend of MC predictions but no one gives a precise description of data.

# Conclusions

**CMS** two independent methods and subdetectors for the **total inelastic cross section**.

**ATLAS** two measurements:

- 1) **total inelastic cross section** (MBTS counting)
- 2) **differential inelastic cross section** (rapidity gaps)

**ATLAS and CMS measured the inelastic cross section in the kinematic range  $\xi > 5 \times 10^{-6}$  then extrapolated to the full range:**

- agreement for  $\sigma_{\text{inel}}(\xi > 5 \times 10^{-6})$ ;
- extrapolations to total inelastic cross section rely entirely on theoretical models  $\rightarrow$  more uncertainties.

Future progresses:

direct measurement of  $\sigma_{\text{inel}}$  via  $\sigma_{\text{tot}}$  and  $\sigma_{\text{el}}$  ongoing with ALFA.

*Back up  
slides*

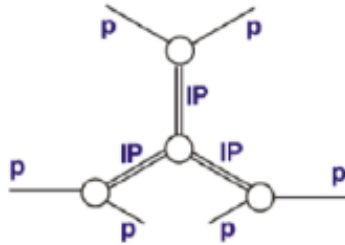


# Diffractive Physics

## Theoretically

1) Interactions where beam particles emerge intact or dissociated into low mass states.

2) Interactions mediated by t-channel exchange ladder of gluons with the quantum numbers of the vacuum (color singlet exchange called “Pomeron”).



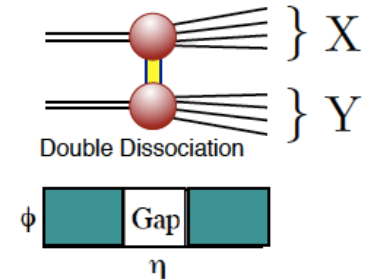
Diffractive physics not yet completely described by QCD. Used phenomenological approaches based on QCD

Diffractive cross section modeled using Regge phenomenology.

Different models used in the Monte Carlo simulations: Ryskin, Martin and Khoze (RMK); Schuler and Sjöstrand; Bruni and Ingelman; Berger and Streng; Donnachie and Landshoff; etc etc...

## Experimentally

Kinematic variable: mass of diffractive system:  $M_{X(Y)}$ , or  $\xi_{X(Y)} \equiv M_{X(Y)}^2/s$  (fractional squared momentum loss).



Total cross section not directly measured by ATLAS and CMS yet.

Direct measurements of  $M_{X(Y)}$  difficult: produced particles escape in the beam-pipe. ATLAS/CMS central detectors sensitive to high mass diffraction; **low mass diffractive dissociation not directly observable.**

Diffractive processes lead to **final state particles separated by large rapidity gaps**: region of no activity (particle production suppressed).

Link between  $M_X$  and rapidity gap  $\Delta \eta$ :  
 $\Delta \eta = \ln s/M_X^2 \sim - \ln \xi_X$ .

# Analysis Strategy

## CMS

### Total inelastic cross section

$L_{\text{int}} = 2.78 \mu\text{b}^{-1}$ , 7 runs in 2010.

$\mu_{\text{mean}} \in [0.007; 0.1]$

High statistics, systematic effect due to pile up.

1) Hits in forward calorimeters:  
kinematic limit not geometrical but  
selection efficiency based:

$$\xi = M_X^2/s > 5 \cdot 10^{-6}$$

(i.e: 5 GeV energy deposited in HF)

2) Visible cross section selecting events  
with at least 1 track.

Inelastic cross section extrapolated at  
full range using MC.

## ATLAS

### 1. Total inelastic cross section

$L_{\text{int}} = 20.3 \mu\text{b}^{-1}$ , single fill in 2010

$\mu_{\text{mean}} = 0.01$ .

Low statistics, no correction for pile  
up.

Limits on measurements due to  
detector acceptance:

$$|\eta| < 4.9 \rightarrow \xi = M_X^2/s > 5 \cdot 10^{-6}$$

(i.e  $M_X > 15.7 \text{ GeV}$ )

Inelastic cross section extrapolated at  
full range using MC.

### 2. Differential cross section

$L_{\text{int}} = 7.1 \pm 0.2 \mu\text{b}^{-1}$ , single fill in 2010.

$\mu_{\text{mean}} = 0.01$  (negligible pile up).

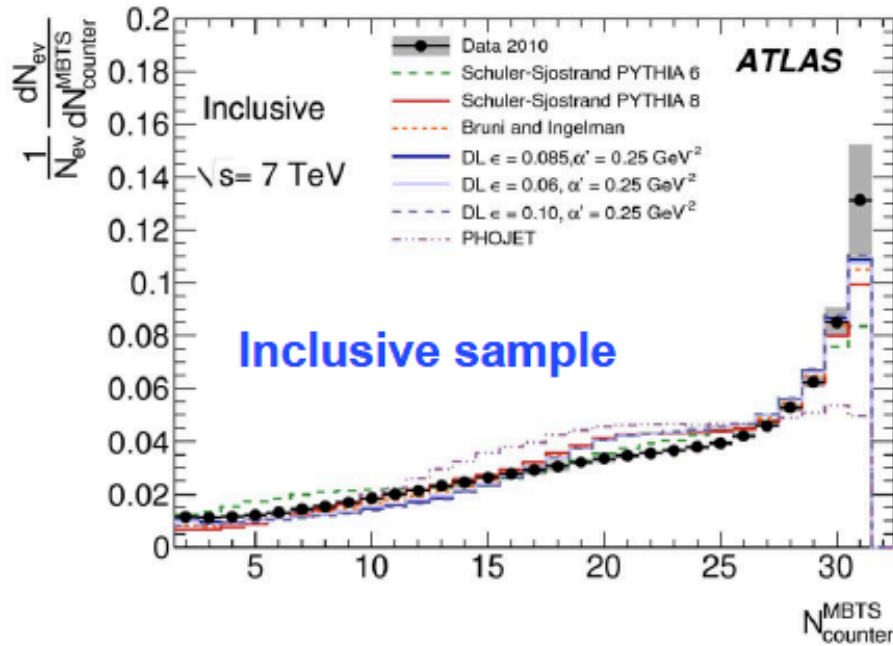
$d\sigma/d\xi$  as function of  $\xi$ .

# ATLAS: MBTS counting

# MC cross section models

Process	cross section (mb)	
	PYTHIA	PHOJET
non-diffractive	48.5	61.6
single diffractive dissociation	13.7	10.7
double diffractive dissociation	9.3	3.9
central diffractive dissociation	-	1.1
inelastic	71.5	77.3
	fractional contribution (%)	
$f_D$	32.2	20.2
$f_{SD}$	59.6	68.6

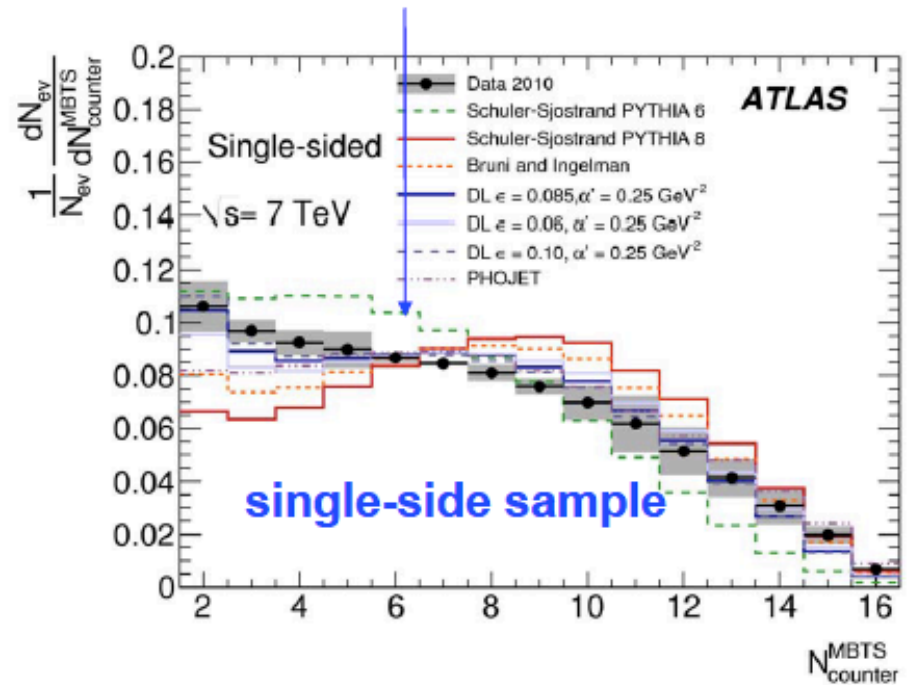
# MBTS multiplicity distribution



**Systematics due to  $\xi$ -distribution**  
**Taken from maximum difference**  
**between models**

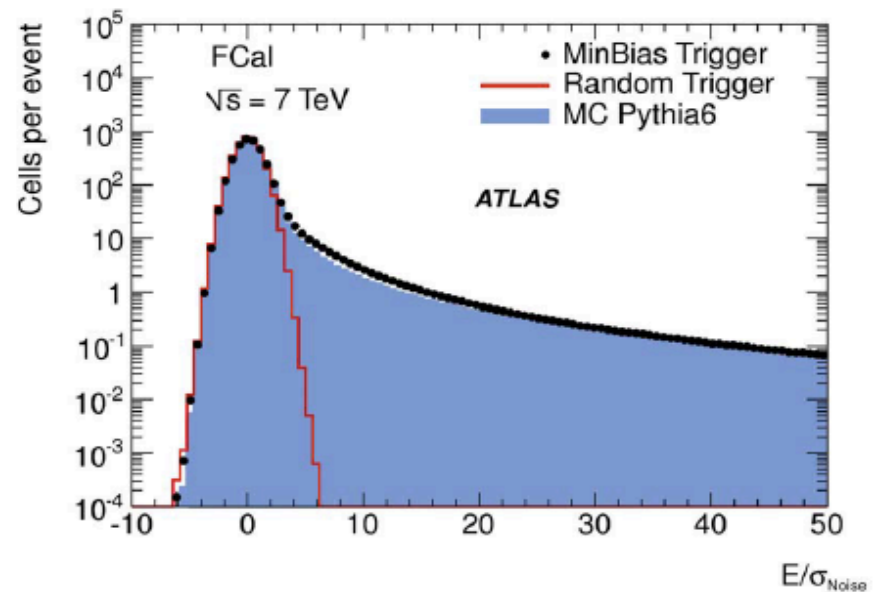
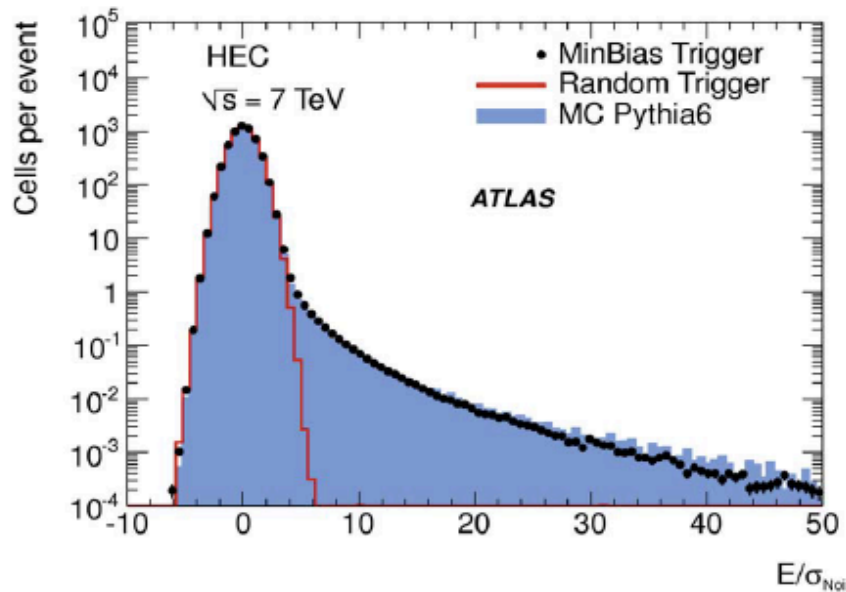
None of the generators is perfect but data lie between the models at low multiplicity

**Donnachie-Landshoff describes well single-side sample**



# Choose threshold in $E_{\text{CaloCell}}$

- Crucial to define what activity in  $\Delta\eta$ -ring is
  - tails in noise distributions: optimize threshold
  - $S = E_{\text{CaloCell}} / \sigma_{\text{noise}} > 4.8\text{-}5.8$  depending on  $\eta$ -ring
- Data vs MC: good understanding of noise over 7 orders of magnitude



# Comparison of the inelastic cross section with prediction

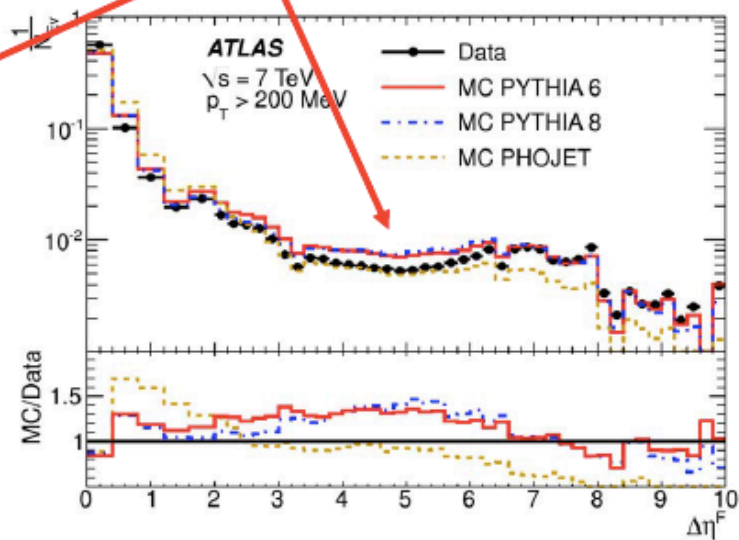
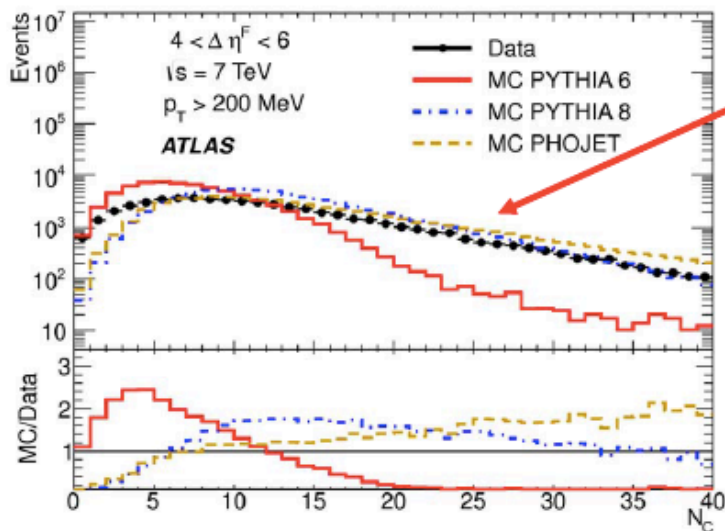
**Table 2 | Comparisons of the inelastic cross-section with predictions.**

$\sigma(\xi > 5 \times 10^{-6})$ (mb)	
ATLAS Data 2010	$60.33 \pm 2.10$ (exp.)
Schuler and Sjöstrand	66.4
Phojet	74.2
Ryskin <i>et al.</i>	51.8-56.2
$\sigma(\xi > m_p^2/s)$ (mb)	
ATLAS Data 2010	$69.1 \pm 2.4$ (exp.) $\pm 6.9$ (extr.)
Schuler and Sjöstrand	71.5
Phojet	77.3
Block and Halzen	$69.0 \pm 1.3$
Ryskin <i>et al.</i>	65.2-67.1
Gotsman <i>et al.</i>	68
Achilli <i>et al.</i>	60-75

Measurement and theoretical predictions of the inelastic cross-section for the restricted kinematic range,  $\xi > 5 \times 10^{-6}$ , and for the full kinematic range,  $\xi > m_p^2/s$ . The experimental uncertainty (exp.) includes the statistical, systematic and luminosity uncertainties. The extrapolation uncertainty (extr.) only applies to the full kinematic range and is listed separately.

# Optimize the MC for data unfolding

- Default MC(s) tuned based on existing measurements:
  - $f_D$  based on previously described ATLAS result
  - $\sigma_{DD}/\sigma_{SC}$  and  $\sigma_{CD}/\sigma_{SD}$  based on Tevatron results
- Tuned-MC vs uncorrected-data on distributions used for data correction: not perfect BUT acceptable (best PYTHIA8 )

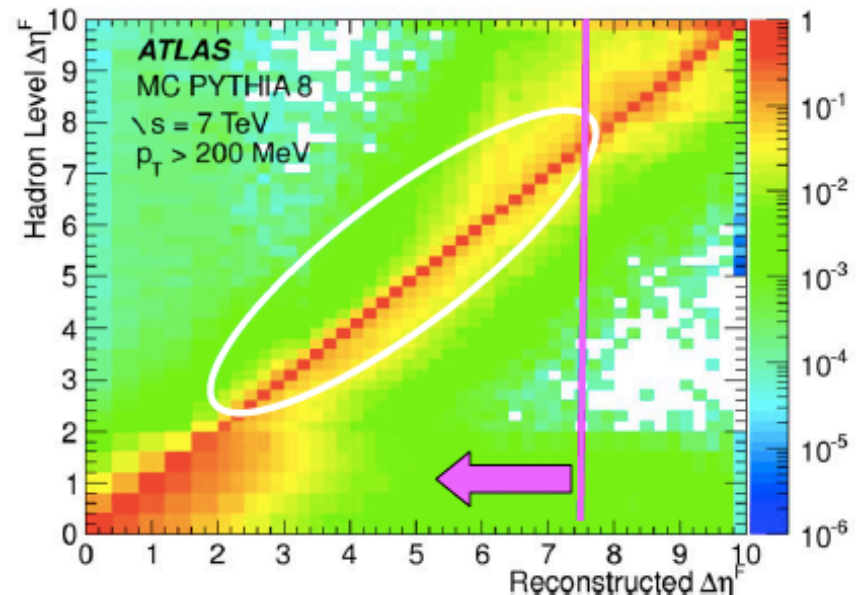




# Experimental Effect / Systematics

- Beam-induced background subtracted (0.2%)
- MBTS efficiency correction ( $\epsilon_{\text{MBTS}} > \sim 95\%$ )
- Migration between reconstructed and hadron-levels
  - Unfolding procedure based on Bayesian method
  - Unfolding matrix approximatively diagonal (small migration in interesting  $\Delta\eta^F$  region)
  - Systematic uncertainty:
    - $< 8\%$  ( $\Delta\eta^F > 3$ )
    - $\sim 20\%$  ( $\Delta\eta^F \sim 1.5$ )
    - $\sim 10\%$  ( $\Delta\eta^F < \sim 1$ )
  - Dominated by  $E_{\text{caloCell}}$

and MC modelling

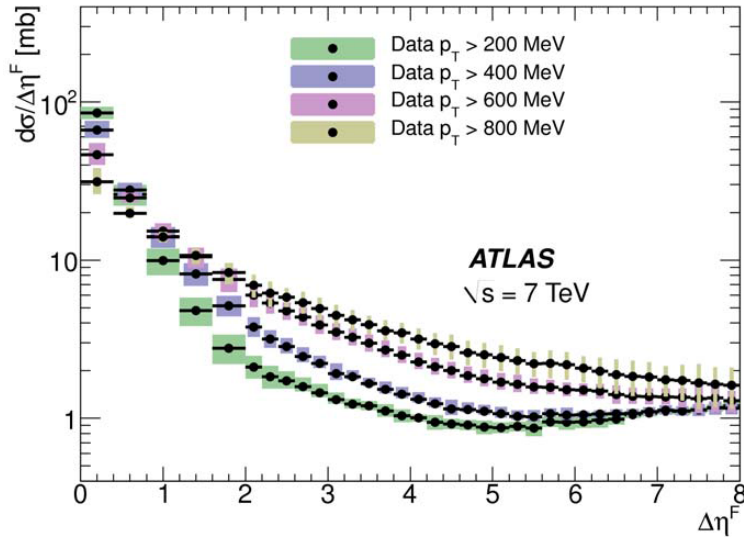


# MC prediction

- $\sigma(s)$ 
  - $s^{\alpha(0)-1}$  where  $\alpha(0)$  is the IP-intercept
  - $\ln(s)$
- Predicted values (ND+SD+DD+CD)
  - PYTHIA:  $48.5+13.7+9.3+0 = 71.5$  mb
  - PHOJET:  $61.6+10.7+3.9+1.1 = 77.3$  mb
- $\xi$ -dependence
  - Schuler and Sjöstrand (default PYTHIA): flat
  - Donnachie-Landshoff (DL):  $1/\xi^{\alpha(0)}$ ,  $\alpha(0)=1.085$ ,  $\alpha'=0.25$   $\text{GeV}^{-2}$  (default model in the analysis)
  - PHOJET: decrease with decreasing  $\xi$

# **ATLAS: Rapidity Gap**

# Hadronization Fluctuation: Uncertainty varying $p_T^{\text{cut}}$

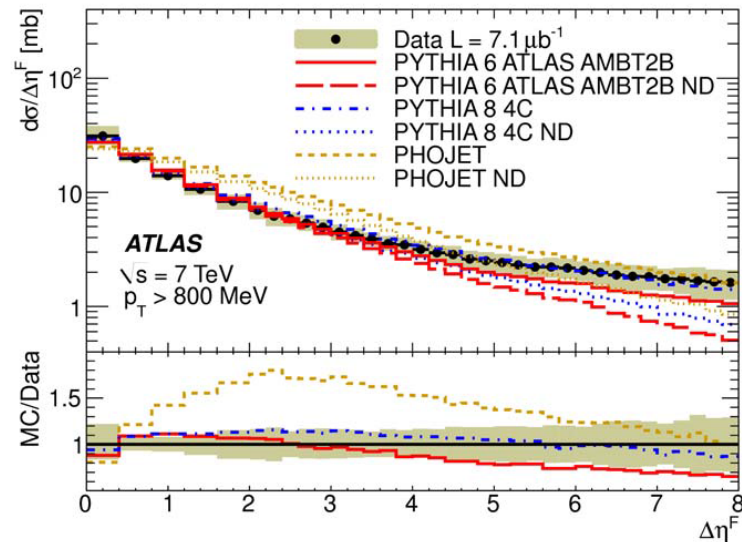
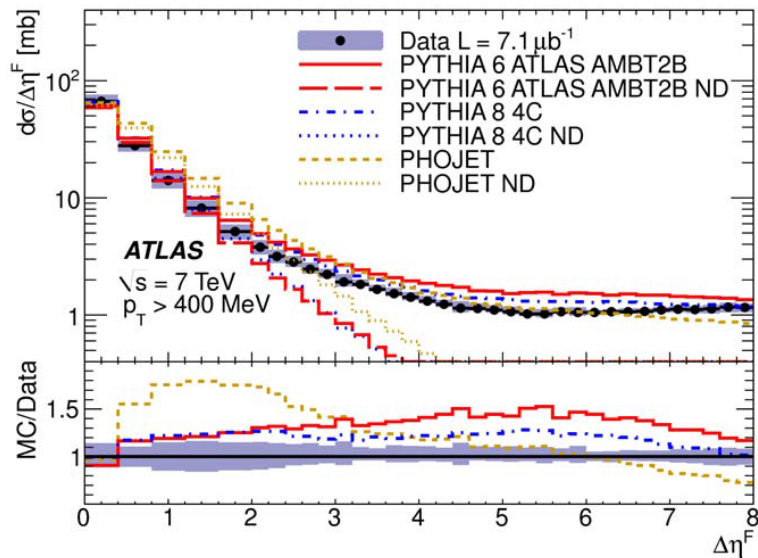


Test MC prediction on hadronization fluctuations at high  $\Delta\eta^F$ .

All models predict by increasing  $p_T$ :

- larger ND component at high  $\Delta\eta^F$ ;
- ND and Diffractive component become similar.

PYTHIA8 better in describing both shape and absolute value.



# Pomeron-flux Parameterization

Flatness at large  $\Delta\eta^F \rightarrow$  Pomeron intercept close to 1.  $\alpha_{IP}(t) = \alpha_{IP}(0) + \alpha'_{IP} t$   
 Increase at large  $\Delta\eta^F$  due to  $\alpha_{IP(0)} > 1$ .  
 In triple Pomeron Regge-model, slope of differential cross section sensitive to Pomeron intercept value:

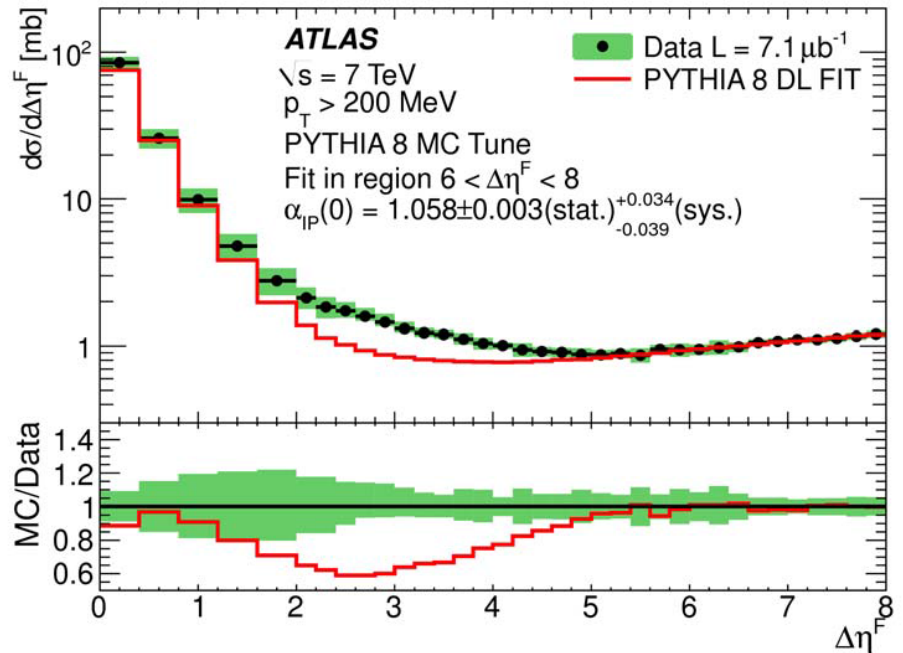
SD differential cross section  $\frac{d\sigma}{dt dM_X^2} = G_{3IP}(0) s^{2\alpha_{IP}(t)-2} (M_X^2)^{\alpha_{IP}(0)-2\alpha_{IP}(t)} f(t)$  Exponential (at fixed energy  $s$  and  $M_X$ )

Coupling

- Best choice of Pomeron intercept:
- cleanest diffractive region  $\Delta\eta^F > 6$
  - PYTHIA8 + Donnachie-Landshoff flux parameterization;
  - varying  $\alpha_{IP}(0)$ ;
  - best estimate:  $\alpha_{IP}(0) = 1.058(40)$

Good description of data at  $\Delta\eta^F > 5$  and  $\Delta\eta^F < 2$ .

- For  $2 < \Delta\eta^F < 5$  discrepancy:
- missing CD component in PYTHIA;
  - uncertainty in modeling large hadronization fluctuations in ND.



# MC prediction

- SD x-sect. expressed as a triple pomeron 3IP amplitude (PYTHIA and PHOJET)
  - $\frac{dt}{dM_x^2} = G_{3IP}(0) s^{2IP(t)-2} (M_x^2)^{\alpha P(0)-2\alpha P(t)} f(t)$ 
    - $G_{3IP}(0)$  = product of couplings
    - $\alpha P(0)-2$   
 $\alpha P(t)$  is IP-trajectory
    - $f(t) = \exp(B(s, M_x^2)t)$
- $\xi$ -dependence: ( $d\sigma/d\ln\xi \sim d\sigma/d\Delta\eta$ )
  - Schuler and Sjostrand (default) :  $\alpha P(0) = 1$ ,  $d\sigma/d\ln\xi \sim \text{const}$
  - Bruni-Ingelmann: double exponential in t-dependence
  - Donnachie-Landshoff:  $\alpha(0)=1.085, \alpha'=0.25 \text{ GeV}^{-2}$
- Tuned MC: each model with respective value for  $f_D$  + CFD constraints on  $f_{DD}/f_{SD}$

# CMS: HF counting

Generator	Efficiency $\epsilon_{\xi}$	
	4 GeV	5 GeV
PYTHIA 6 ( $\xi > 5 \times 10^{-6}$ )	98.7 $\pm$ 0.6 %	97.5 $\pm$ 0.6 %
PYTHIA 8 ( $\xi > 5 \times 10^{-6}$ )	99.7 $\pm$ 0.2 %	99.3 $\pm$ 0.2 %
PHOJET ( $\xi > 5 \times 10^{-6}$ )	99.4 $\pm$ 0.2 %	99.1 $\pm$ 0.2 %

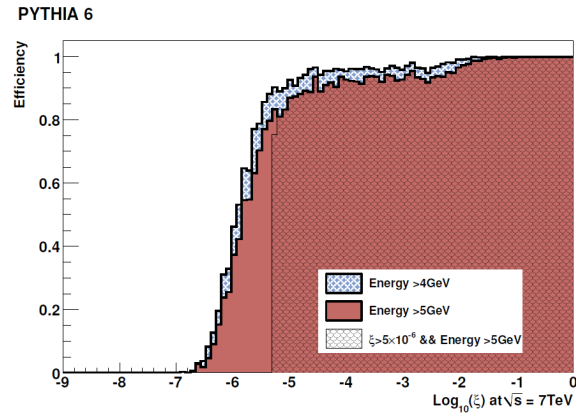
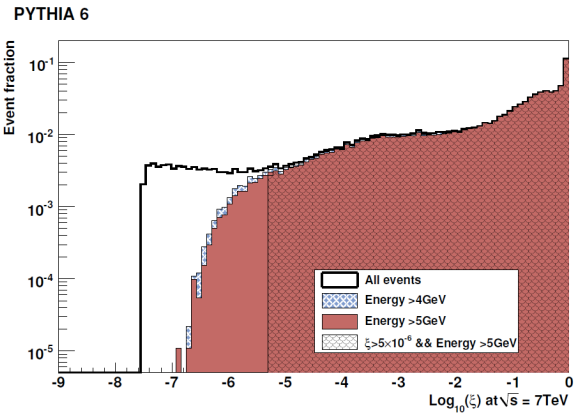
Generator	$f_{\xi}$	
	4 GeV	5 GeV
PYTHIA 6	0.0234	0.0200
PYTHIA 8	0.0256	0.0205
PHOJET	0.0143	0.0118

Run No.	$\lambda$	$f_{pu}$
132 601	(0.64 $\pm$ 0.01)%	0.0032 $\pm$ 0.0001
132 599	(0.78 $\pm$ 0.01)%	0.0039 $\pm$ 0.0001
133 877	(1.74 $\pm$ 0.02)%	0.0087 $\pm$ 0.0001
133 874	(3.34 $\pm$ 0.05)%	0.0166 $\pm$ 0.0002
137 027	(4.59 $\pm$ 0.17)%	0.0228 $\pm$ 0.0009
135 575	(8.41 $\pm$ 0.04)%	0.0415 $\pm$ 0.0002
135 175	(9.98 $\pm$ 0.05)%	0.0491 $\pm$ 0.0003

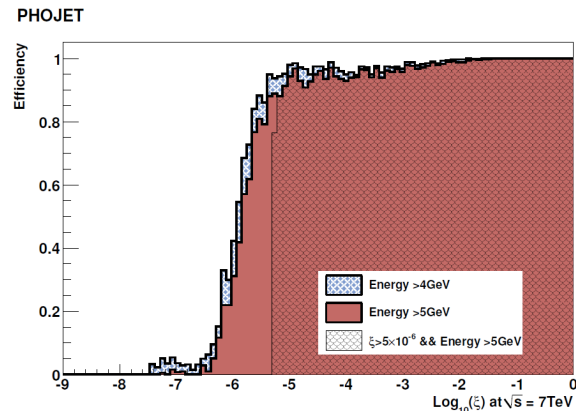
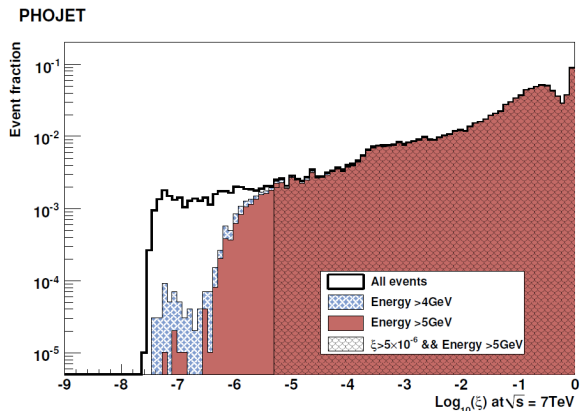
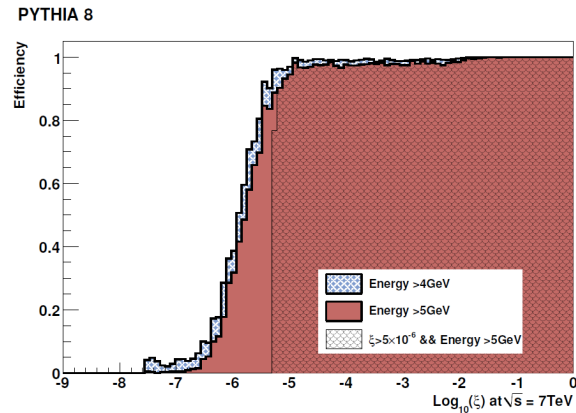
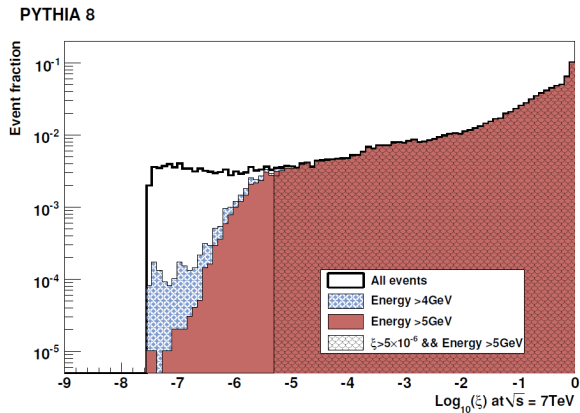
Generator	$\epsilon_{\xi}$	$f_{\xi}$	Extrapolation Factor $\frac{\epsilon_{\xi}}{(1-f_{\xi})\epsilon_{inel}}$
PYTHIA 6	0.995	0.0272	1.0911
PYTHIA 8	0.999	0.0263	1.0904
PHOJET	0.997	0.0146	1.0402
SIBYLL	0.999	0.0173	1.0548
EPOS	0.997	0.0064	1.0498
QGSJET-II	0.996	0.0281	1.0977
Average	0.997	0.0200	1.0707

$$\frac{\epsilon_{\xi}}{\epsilon_{inel}(1-f_{\xi})}$$

# Event Selection Efficiency



3 different generator  
and for two threshold  
energy





# CMS: pile up counting

To select vertices with at least 2 track  $\rightarrow$  NDOF  $>$  0.5

$$NDOF = 2 * \sum_{tracks} (weights) - 3 \quad \text{weight} \in [0;1] \text{ (1=perfect track)}$$

# Vertex Definition

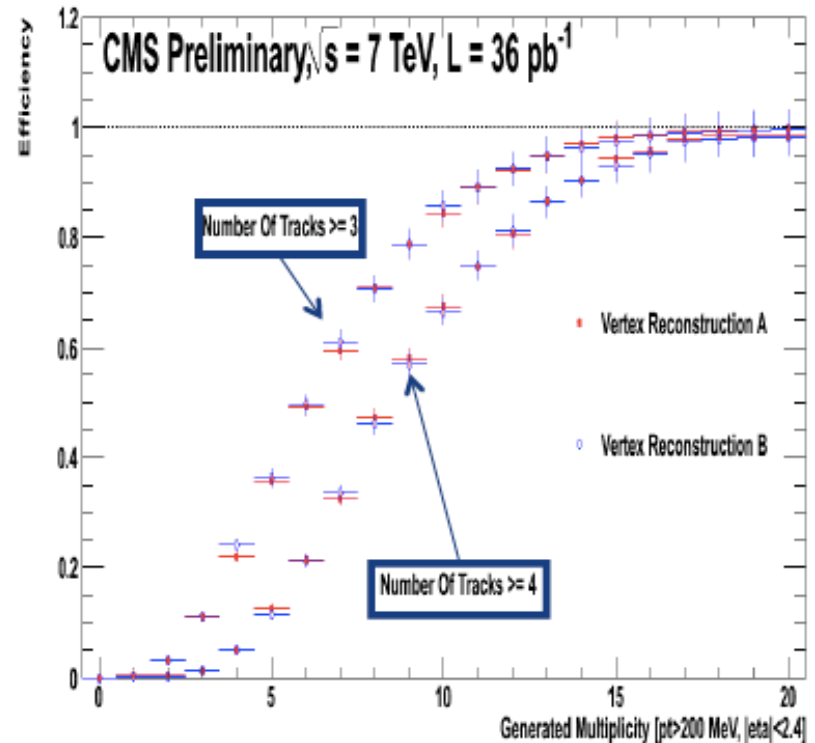
- **We select PU event large enough to make a vertex:**
  - We count vertexes requiring at least 3 tracks with  $|\eta| < 2.4$  &&  $p_t > 200$  MeV
  - Each track should have at least 2 pixel hits && 5 Strip hits
- **We define “real” those vertexes generated in pp scattering and “fake” those created by other mechanisms. Fake come mostly from:**
  - Real secondary vertexes (i.e. generated by long lived particles)
  - Split secondary vertexes (i.e generated by the vertex algorithm splitting a single vertex in two)

**Fake vertexes have been studied with Pythia generated without PU (i.e. at most one interaction -> secondary vertex is fake by definition)**

**Fake vertexes rate  $\sim 1.5 \cdot 10^{-3}$**

# Vertex reconstruction efficiency

- Using a full GEANT simulation of the tracker detector we studied the vertex reconstruction efficiency.
- The most important parameter is the vertex multiplicity:  
**vertexes with < 17 tracks are not always reconstructed**
- The algorithm reconstructs vertexes separated by more than 0.06 mm. The “blind distance” is largely independent of the number of tracks in the vertexes.

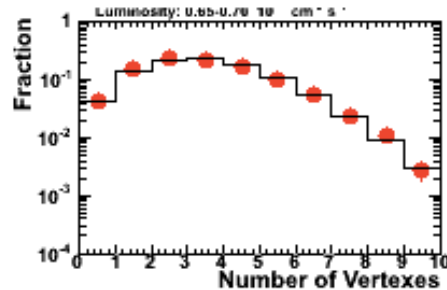
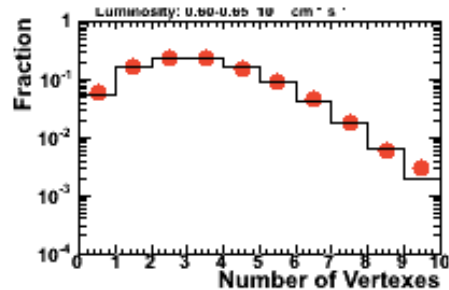
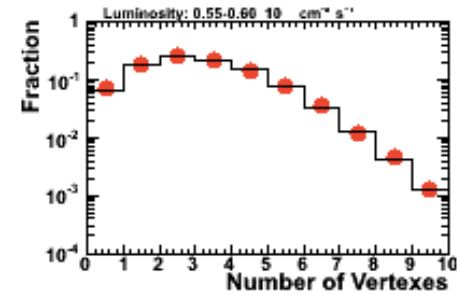
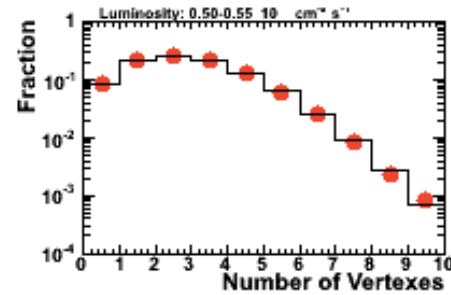
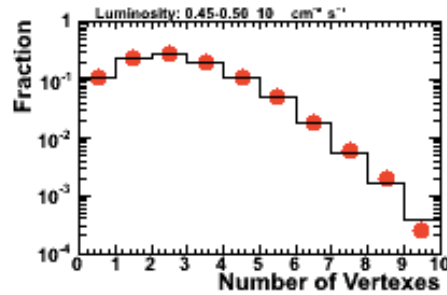
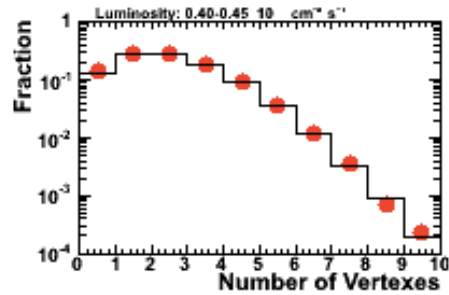
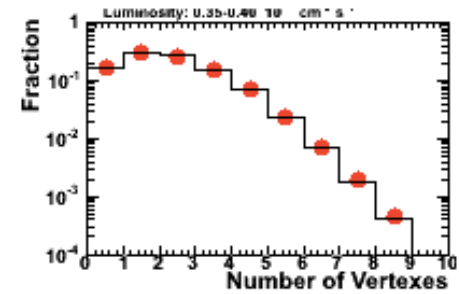
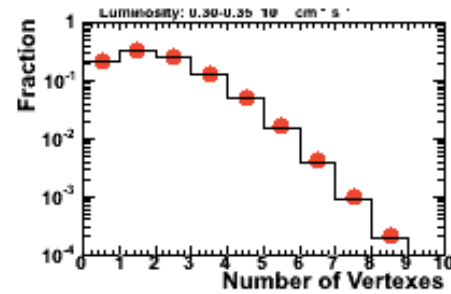
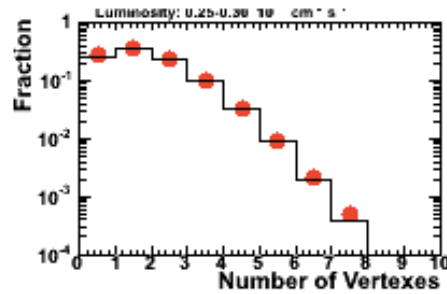
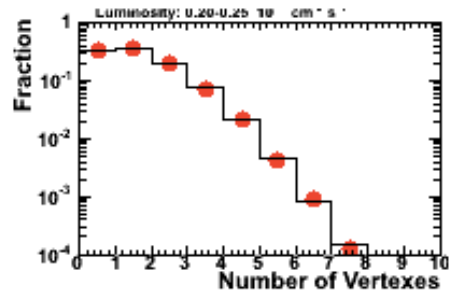
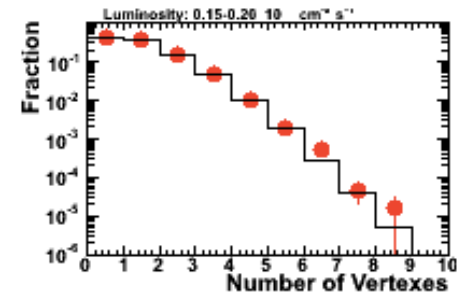
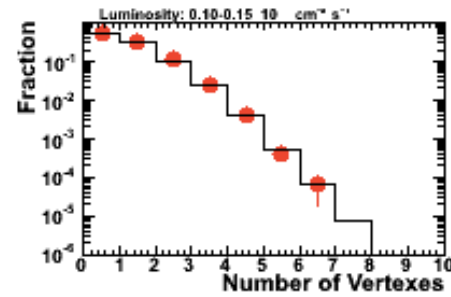
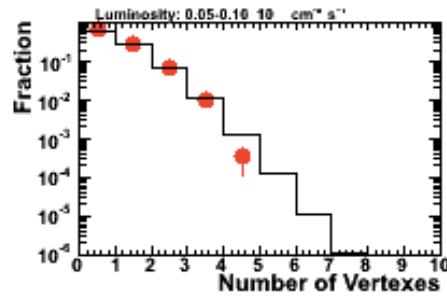


**Need to correct the PU distribution for the missing fraction of events at low multiplicity and for vertex merging**

# Vertex reconstruction efficiency

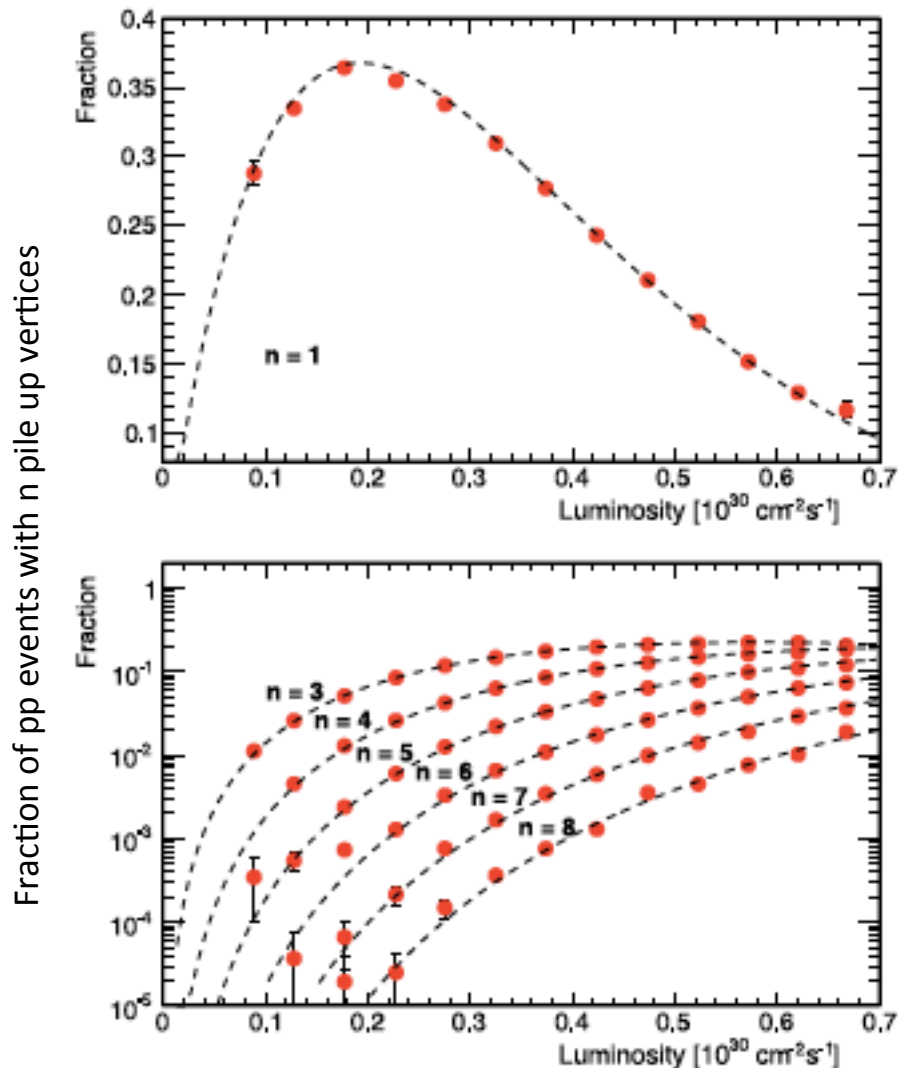
CMS Preliminary

$\sqrt{s} = 7 \text{ TeV}, L = 36 \text{ pb}^{-1}$



● Measured  
— MC - Predicted

# Pile Up Distribution vs Luminosity



- The expected distribution of pile up interactions calculated for a specific luminosity interval;
- MC simulation reweighted to generate a distribution matching the calculated one;
- The generated pile up distributions for inclusive interactions with  $>1$ ,  $>2$  and  $>3$  tracks each with  $p_T > 200 \text{ MeV}$  and  $|\eta| < 2.4$  obtained from reweighted MC;
- bin-by-bin correction computed using ratio reconstructed to generated MC pile up distributions for the three inclusive sets on events.

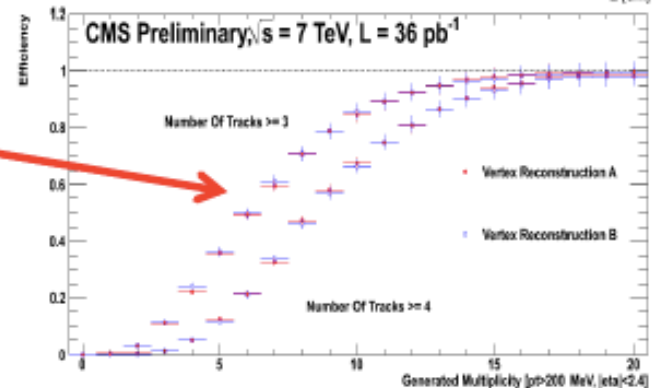
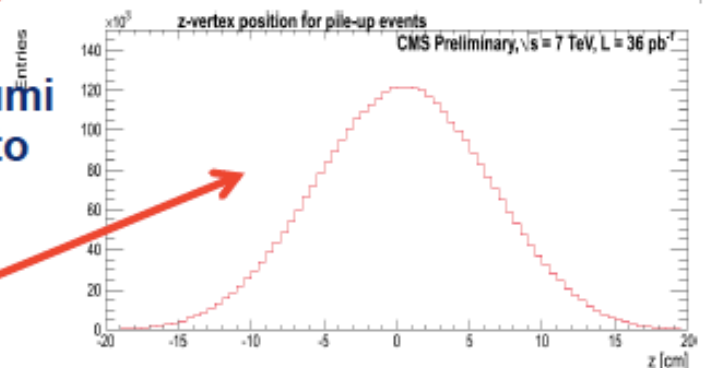
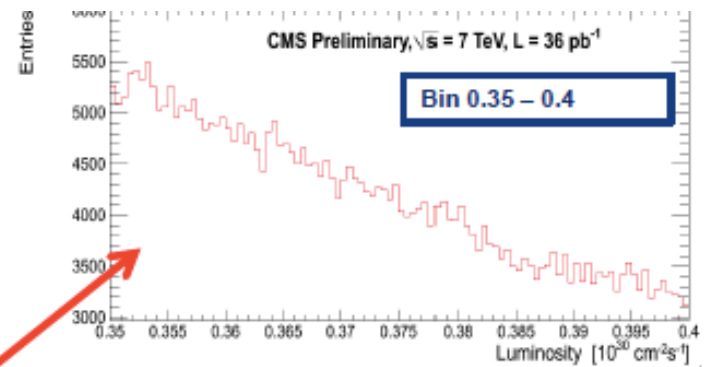
Good agreement with Poisson fit.

# Unfolding

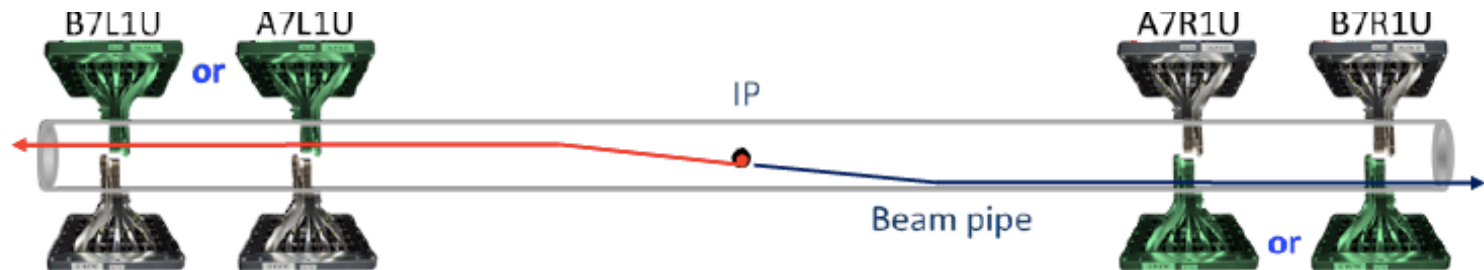
The visible number of vertexes needs to be corrected to obtain the “real” number. This is done in luminosity bins (14).

An unfolding technique is used, according to the following steps:

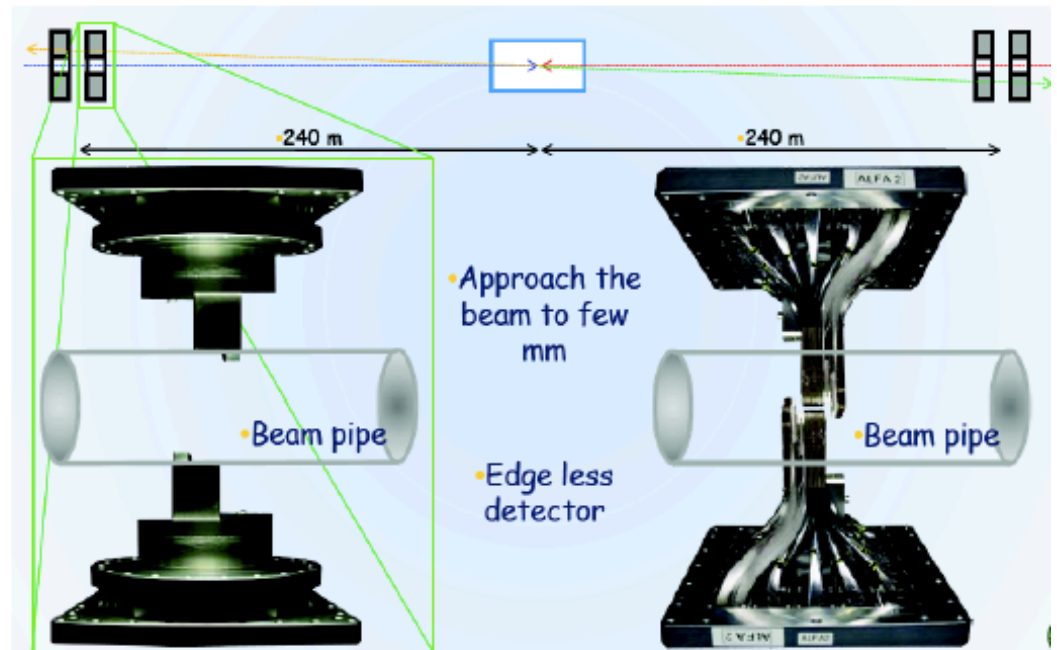
- 1) Generate the “true” vertex distribution in luminosity bins (convolution of measured lumi + poisson). Use the true vertex distribution to generate events with  $n$  vertexes
- 2) Assign to each of the generated vertex a multiplicity and a position in  $z$  according to the data distribution
- 3) For vertexes with low multiplicity decides whether or not they are selected. Vertexes closer together than 0.06 cm are merged
- 4) Fill the calculated “visible” distribution



# Other Measurements: ALFA



- Modified optics needed ( $\beta^* > 90\text{m}$ )
- Trigger on left-right coincidence (elastic)
- Prescaled triggers for diffraction
- First data taking October 2011
  - Analysis ongoing
- Loose cuts on back-to-back topology



# Other Measurements: TOTEM

TOTEM has measured the differential cross-section for elastic proton-proton scattering at the LHC energy of  $\sqrt{s} = 7$  TeV analysing data from a short run with dedicated large  $\beta^*$  optics. A single exponential fit with a slope  $B = (20.1 \pm 0.2^{\text{stat}} \pm 0.3^{\text{syst}}) \text{ GeV}^{-2}$  describes the range of the four-momentum transfer squared  $|t|$  from 0.02 to  $0.33 \text{ GeV}^2$ . After the extrapolation to  $|t| = 0$ , a total elastic scattering cross-section of  $(24.8 \pm 0.2^{\text{stat}} \pm 1.2^{\text{syst}}) \text{ mb}$  was obtained. Applying the optical theorem and using the luminosity measurement from CMS, a total proton-proton cross-section of  $(98.3 \pm 0.2^{\text{stat}} \pm 2.8^{\text{syst}}) \text{ mb}$  was deduced which is in good agreement with the expectation from the overall fit of previously measured data over a large range of center-of-mass energies. From the total and elastic pp cross-section measurements, an inelastic pp cross-section of  $(73.5 \pm 0.6^{\text{stat}} \pm 1.3^{\text{syst}}) \text{ mb}$  was inferred.

**Extrapolation to  $t = 0$**  The elastic differential cross-section has been measured down to  $|t| = 2 \times 10^{-2} \text{ GeV}^2$ . The data were then extrapolated to  $t = 0$  assuming the functional form

$$\frac{d\sigma_{\text{el}}}{dt} = \left. \frac{d\sigma_{\text{el}}}{dt} \right|_{t=0} e^{-B|t|}. \quad (3)$$

The total proton-proton cross-section is related to the elastic cross-section via the optical theorem

$$\sigma_{\text{tot}}^2 = \frac{16\pi(\hbar c)^2}{1 + \rho^2} \left. \frac{d\sigma_{\text{el}}}{dt} \right|_{t=0}. \quad (4)$$

Taking the COMPETE prediction [30] of  $0.14^{+0.01}_{-0.08}$  for the parameter  $\rho = \frac{\Re[f_{\text{el}}(0)]}{\Im[f_{\text{el}}(0)]}$ , where  $f_{\text{el}}(0)$  is the forward nuclear elastic amplitude,  $\sigma_{\text{tot}}$  was thus determined to be

$$\sigma_{\text{tot}} = \left( 98.3 \pm 0.2(\text{stat}) \begin{array}{l} +2.8 \\ -2.7 \end{array} (\text{syst}) \right) \text{ mb}. \quad (5)$$

The errors are dominated by the extrapolation to  $t = 0$  and the luminosity uncertainty.



Table 1: Results of the TOTEM measurements at the LHC energy of  $\sqrt{s} = 7$  TeV.

	Statistical uncertainties	Systematic uncertainties	Result
$t$	$\pm[3.4 \div 11.9]\%$ single measurement <sup>(*)</sup>	$\pm[0.6 \div 1.8]\%$ optics $\pm < 1\%$ alignment	
$\frac{d\sigma}{dt}$	5% / bin	$\pm 4\%$ luminosity $\pm 1\%$ analysis $\pm 0.7\%$ unfolding	
B	$\pm 1\%$	$\pm 1\%$ $t$ -scale $\pm 0.7\%$ unfolding	$(20.1 \pm 0.2^{\text{stat}} \pm 0.3^{\text{syst}}) \text{ GeV}^{-2}$
$\frac{d\sigma}{dt} _{t=0}$	$\pm 0.3\%$	$\pm 0.3\%$ optics $\pm 4\%$ luminosity $\pm 1\%$ analysis	$(503.7 \pm 1.5^{\text{stat}} \pm 26.7^{\text{syst}}) \text{ mb/GeV}^2$
$\int \frac{d\sigma}{dt} dt$	$\pm 0.8\%$ extrapolation	$\pm 4\%$ luminosity $\pm 1\%$ analysis	
$\sigma_{\text{tot}}$	$\pm 0.2\%$	$\left(\begin{smallmatrix} +0.8\% \\ -0.2\% \end{smallmatrix}\right)^{(\rho)} \pm 2.7\%$	$(98.3 \pm 0.2^{\text{stat}} \pm 2.8^{\text{syst}}) \text{ mb}$
$\sigma_{\text{el}} = \int \frac{d\sigma}{dt} dt$	$\pm 0.8\%$	$\pm 5\%$	$(24.8 \pm 0.2^{\text{stat}} \pm 1.2^{\text{syst}}) \text{ mb}$
$\sigma_{\text{inel}}$	$\pm 0.8\%$	$\left(\begin{smallmatrix} +2.4\% \\ -1.8\% \end{smallmatrix}\right)$	$(73.5 \pm 0.6^{\text{stat}} \pm 1.8^{\text{syst}}) \text{ mb}$
$\sigma_{\text{inel}}$ (CMS)			$(68.0 \pm 2.0^{\text{syst}} \pm 2.4^{\text{lumi}} \pm 4^{\text{extrap}}) \text{ mb}$
$\sigma_{\text{inel}}$ (ATLAS)			$(69.4 \pm 2.4^{\text{exp}} \pm 6.9^{\text{extrap}}) \text{ mb}$
$\sigma_{\text{inel}}$ (ALICE)			$(72.7 \pm 1.1^{\text{model}} \pm 5.1^{\text{lumi}}) \text{ mb}$

<sup>(\*)</sup>corrected after unfolding

analysis (includes tagging, acceptance, efficiency, background)

